JAERI-M
82-075

SCTF CORE-I TEST RESULTS (SYSTEM PRESSURE EFFECTS ON REFLOODING PHENOMENA)

July 1982

Hiromichi ADACHI, Yukio SUDO, Takamichi IWAMURA
Masahiro OSAKABE, Akira OHNUKI and Kemmei HIRANO

日本原子力研究所
Japan Atomic Energy Research Institute

JAERI-Mレポートは，日本原子力研究所が不定期に公刊している研究報告書です。
入手の問合わせは，日本原子力研究所技術情報部情報資料課（〒319-11茨城県那珂郡東海村）あて，お申しこしください。なお，このほかに財団法人原子力弘済会資料センター（〒319-11茨城県那珂郡東海村日本原子力研究所内）で複写による実費頒布をおこなっております。

JAERI-M reports are issued irregularly.
Inquiries about availability of the reports should be addressed to Information Section, Division of Technical Information, Japan Atomic Energy Research Institute, Tokai-mura, Naka-gun, Ibaraki-ken 319-11, Japan.

編集兼発行　日本原子力研究所
印　　刷　㈱高野高速印刷

SCTF Core-I Test Results
(System Pressure Effects on Reflooding Phenomena)

Hiromichi ADACHI, Yukio SUDO, Takamichi IWAMURA
Masahiro OSAKABE, Akira OHNUKI and Kemmei HIRANO

Division of Nuclear Safety Research,
Tokai Research Establishment, JAERI

(Received June 1, 1982)

The Slab Core Test Facility (SCTF) of Japan Atomic Energy Research Institute (JAERI) was constructed to investigate two-dimensional thermo-hydrodynamics in the core and the communication in fluid behavior between the core and the upper plenum during the last part of blowdown, refill and reflood phases of a posturated loss-of-coolant accident (LOCA) of a pressurized water reactor (PWR).

In the present report, effects of system pressure on reflooding phenomena shall be discussed based on the data of Tests S1-SH2, S1-01 and S1-02 which are the parameteris tests for system pressure effects belonging to the SCTF Core-I forced flooding test series. Major items discussed in this report are (1) hydrodynamic behavior in the system, (2) core thermal behavior, (3) core heat transfer and (4) two-dimensional hydrodynamic behavior in the pressure vessel including the core.

Keywords: Reflood, System Pressure, SCTF, Fluid Behavior, Core, Thermal Behavior, Heat Transfer, 2-Dimensional Fluid Dynamics, ECCS

The work was performed under contract with the Atomic Energy Bureau of Science and Technology Agency of Japan.

This paper was presented at the Ninth Water Reactor Safety research Information Meeting, Gaithersburg, Maryland, October 26-30, 1981.

平板炉心再冠水試験・第1次模擬炉心試験結果
（系圧力の再冠水現象に及ぼす影響）

日本原子力研究所東海研究所安全工学部
安達　公道・数土　幸夫・岩村　公道
刑部　真弘・大貫　　晃・平野　見明

（1982年6月1日受理）

日本原子力研究所では，加圧水型原子炉（Pressurized Water Reactor，略称PWR）の冷却材喪失事故（Loss－of－Coolant Accident，略称LOCA）時の，ブローダウン過程末期から，リフィル，再冠水過程における，炉心二次元熱水力挙動や，炉心の流体挙動と上部プレナムの流体挙動との間の相互干渉などを解明するために，平板炉心試験装置（Slab Core Test Facility，略称SCTF）を製作した。

本報告書では，第1次模擬炉心を用いた強制注入試験シリーズのうち，系圧力の効果を調べた試験S1－SH2，S1－01およびS1－02のデータを用いて，再冠水現象に及ぼす系圧力の影響を論ずる。本報告書で論ずる主な検討項目は，(1)システム内の流体挙動，(2)炉心の熱的挙動，(3)炉心熱伝達，および(4)炉心を含む圧力容器内の二次元流体挙動などである。

本報告書は，電源開発促進対策特別会計法に基づき，科学技術庁からの受託によって行った研究の成果である。また，本報告書は，米国原子力規制委員会主催の第9回軽水炉安全性研究情報会議（1981年10月26日～30日）で発表された。

Contents

目　　次

List of Tables

Lidt of Figures

1. Introduction

The Slab Core Test Facility (SCTF) of Japan Atomic Energy Research Institute (JAERI) was constructed to investigate two-dimensional thermo-hydrodynamics in the core and the communication in fluid behavior between the core and the upper plenum during the last part of blowdown, refill and reflood phases of a postulated loss-of-coolant accident (LOCA) of a pressurized water reactor (PWR).

The SCTF Test Program is being carried out in accordance with the so-called 2D/3D Agreement among the United States (US), Federal Republic of Germany (FRG) and Japan. Coupling tests with the SCTF and the Upper Plenum Test Facility (UPTF) of FRG will be performed in the future as an activity based on the 2D/3D Agreement.

To meet these purposes, the SCTF was designed to simulate the slab shaped part of the actual PWR core with full height, full radius and one bundle width including the corresponding parts of the upper and lower plena and the downcomer, as shown in Fig. 1. Internal structure of the pressure vessel is shown in Fig. 2. Furthermore, simplified primary coolant loops are attached to the SCTF, as shown in Fig. 3.

The simulated core consists of eight electrically heated simulated fuel bundles arranged in a straight line. The total core heating capacity is about 10 MW. Design of each simulated fuel bundle is principally based on that for a Westinghouse 15 × 15 fuel bundle, however, the bundle size is 16 × 16. The No.1 and No.8 bundles are simulated the center and peripheral bundles of an actual core, respectively. The No.3 and No.4 bundles are so-called blockage bundles and all heater rods in these two bundles have blockage sleeves at the midplane for simulation of balooned fuel rods.

In the present report, the effects of system pressure on reflooding phenamena shall be discussed based on the data of Tests S1-SH2 (nominal system pressure: 0.4 MPa), S1-01 (0.2 MPa) and S1-02 (0.15 MPa) which are the parameteric tests for system pressure effects belonging to the SCTF Core-I forced flooding test series. The major test conditions and the chronologies of events in these three tests are given in Table 1 ∿ 3 and Table 4 ∿ 6, respectively.

2. Major Results

(1) Hydrodynamic Behavior in the System

i) To clarify the overall fluid behavior in the system and to estimate quality of the instrumentation, mass balance for each part of the system was investigated. The results are shown in Figs. 4∿6. Very good agreement of integral amount of the injected emergency core cooling (ECC) water with the sum of steam and water discharges from the pressure vessel and accumulated water in the pressure vessel was confirmed. This result suggests the reliability inninstrumentation of these tests on the whole.

ii) Higher carryover water flow rate in the hot leg was measured when the system pressure was lower as shown in Fig. 7, suggesting the effect of higher steam velocity due to the larger specific volume of steam on carryover phenomenon.

(2) Core Thermal Behavior

i) Core thermal behaviors including quench propagation and turnaround behavior of cladding temperature were investigated. Samples of cladding temperature transient are given in Fig. 8.

The higher system pressure gave the shorter quench time, the higher quench temperature and the shorter turnaround time, as shown in Figs. 9 ∿11, respectively. These characteristics can clearly be seen especially in the middle and lower part of the core. However, no significant effect of system pressure on the turnaround temperature was observed, as shown in Fig. 12. Two of the reasons of the small system pressure effect on the turnaround temperature are that cladding temperature at the BOCREC (bottom-of-core recovery) was set nearly equal in the present three tests and in addition temperature rise from the BOCREC to the turnaround point was small.

ii) Quench propagated upward except for the upper part of the core where downward quench propagation was observed, as shown in Figs. 13 and 14.

Downward quench propagation was a random phenomenon and many thermocouples showed earlier quench than the others at the same elevation, as shown in Fig. 15. Downward quench propagation may be caused by cooling effect of deoplets coming from the lower part of the core and water film flowing down from the upper plenum. Effects of the non-heated rods

and the arrangement of the upper plenum structures on quench time of the downward propagated quench are suggested.

iii) As for the upward quench propagation, small effects of radial power distribution of the core on quench time and turnaround temperature were observed, as shown in Figs. 15 and 17, however no significant effect on quench temperature, as shown in Fig. 16. In addition, no significant effect of blockage sleeves on quench behavior was indicated.

iv) Azimuthal distribution of quench time was observed throughout the core, as shown in Fig. 18, suggesting the heat sink effect of the slab wall. This effect should be evaluated quanitatively in the future because the actual PWR does not have such a slab wall as the SCTF.

v) The upward quench propagation velocity showed good agreement with the Murao's correlation(1) at the relatively higher system pressure, as shown in Fig. 19. The murao's correlation, however, gives the different tendency against system pressure in comparison with the test data; therefore, discrepancy between the calculation and the test data increased in the low system pressure condition. It should be pointed out that the test conditions of the present three tests were out of application range of the Murao's correlation, especially in flooding speed and quench temperature.

(3) Core Heat Transfer

i) Heat transfer coefficient at the surface of the heater rods at the same time was higher when system pressure was higher, as shown in Fig. 20. Heat Flux also showed the similar tendency.

ii) Sudo's correlation(2) on film boiling heat transfer gives slightly higher heat transfer coefficient for the upstream of quench front but can be almost satisfactorily applied to the present three tests, as shown in Fig. 20.

(4) Two-Dimensional Hydrodynamic Behavior in the Pressure Vessel including the Core

i) Two-dimensional hydrodynamic behaviors in the pressure vessel including the core were indicated in several kinds of data such as horizontal distribution of differential pressure between the inlet and outlet of the core (Fig. 21), horizontal pressure difference between the No. 1 and No. 8 bundles, (Fig. 23) horizontal distributions of fluid

density in the core, (Figs. 24∿26), water level on the end box tie plates (Fig. 27), pressure drop across the end box tie plates (Fig. 28) and water level on the upper core support plate (Fig. 29).

ii) The two-dimensionality itself was not so large but this does not mean that horizontal component of core fluid velocity was small. For example, the one-dimensional analysis using the Cunningham-Yeh's correlation[3] could not give a good prediction for the horizontal distribution of differential pressure between the inlet and outlet of the core, as shown in Fig. 22. This suggests that flattening of horizontal pressure distribution occurred due to the horizontal component of the core flow.

iii) Pressure drop data across the end box tie plates (Fig. 28) suggests that a downward water flow (fall back) exists at the No.8 bundle in the peripheral region of the core. Similar phenomenon was also seen at the next peripheral No.7 bundle (Data not shown.).

iv) The effect of blockage sleeves on the two-dimensional hydrodynamics in the core was not significant as seen in the present three tests. Final conclusion on this item should, however, be made after the future cold leg injection tests because a forced flooding test has a possibility to overlook the important characters of the reflooding phenomena in the actual PWR.

References

(1) Y. Murao, J. Nucl. Sci. Techno., 15 [12], 875∿885 (1978)

(2) Y. Sudo, J. Nucl. Sci. Techno., 17 [7], 516∿530 (1980)

(3) J. P. Cunningham and H. C. Yeh, Trans. ANS, 17, 369∿370 (1973)

density in the core, (Figs. 24∿26), water level on the end box tie plates (Fig. 27), pressure drop across the end box tie plates (Fig. 28) and water level on the upper core support plate (Fig. 29).

ii) The two-dimensionality itself was not so large but this does not mean that horizontal component of core fluid velocity was small. For example, the one-dimensional analysis using the Cunningham-Yeh's correlation[3] could not give a good prediction for the horizontal distribution of differential pressure between the inlet and outlet of the core, as shown in Fig. 22. This suggests that flattening of horizontal pressure distribution occurred due to the horizontal component of the core flow.

iii) Pressure drop data across the end box tie plates (Fig. 28) suggests that a downward water flow (fall back) exists at the No.8 bundle in the peripheral region of the core. Similar phenomenon was also seen at the next peripheral No.7 bundle (Data not shown.).

iv) The effect of blockage sleeves on the two-dimensional hydrodynamics in the core was not significant as seen in the present three tests. Final conclusion on this item should, however, be made after the future cold leg injection tests because a forced flooding test has a possibility to overlook the important characters of the reflooding phenomena in the actual PWR.

References

(1) Y. Murao, J. Nucl. Sci. Techno., 15 [12], 875∿885 (1978)

(2) Y. Sudo, J. Nucl. Sci. Techno., 17 [7], 516∿530 (1980)

(3) J. P. Cunningham and H. C. Yeh, Trans. ANS, 17, 369∿370 (1973)

Table 1 Test Conditions for Test S1-SH2

TEST TYPE	FORCED FLOODING
INITIAL PRESSURE (CORE CENTER)	0.397 MPA
PRESSURE (CONTAINMENT - II)	0.397 MPA (INITIAL) 0.425 MPA (MAX)
MAX CORE TEMP (AT BOCREC)	973 K (NOMINAL)
POWER HOLDING AFTER ACC INITIATION	5 SEC (NOMINAL)
DECAY CURVE	ANS + ACTINIDES + D.N. FROM 30 SEC (REAC. TIME)
MAX ACC INJ. RATE	20 KG/SEC
LPCI INJ. RATE	11 KG/SEC
MAX CORE INLET SUBCOOLING	14.7 K

Table 2 Test Conditions for Test S1-01

TEST TYPE	FORCED FLOODING
INITIAL PRESSURE (CORE CENTER)	0.198 MPA
PRESSURE (CONTAINMENT - II)	0.195 MPA (INITIAL) 0.218 MPA (MAX)
MAX CORE TEMP (AT BOCREC)	973 K (NOMINAL)
POWER HOLDING AFTER ACC INITIATION	5 SEC (NOMINAL)
DECAY CURVE	ANS + ACTINIDES + D.N. FROM 30 SEC (REAC. TIME)
MAX ACC INJ. RATE	22 KG/SEC
LPCI INJ. RATE	11.4 KG/SEC
MAX CORE INLET SUBCOOLING	15.5 K

Table 3 Test Conditions for Test S1-02

TEST TYPE	FORCED FLOODING
INITIAL PRESSURE (CORE CENTER)	0.150 MPA
PRESSURE (CONTAINMENT - II)	0.150 MPA (INITIAL) 0.169 MPA (MAX)
MAX CORE TEMP (AT BOCREC)	973 K (NOMINAL)
POWER HOLDING AFTER ACC INITIATION	5 SEC (NOMINAL)
DECAY CURVE	ANS + ACTINIDES + D.N. FROM 30 SEC (REAC. TIME)
MAX ACC INJ. RATE	21.4 KG/SEC
LPCI INJ. RATE	10.6 KG/SEC
MAX CORE INLET SUBCOOLING	19.0 K

Table 4 Chronology of Test S1-SH2

	TIME AFTER CORE POWER"ON"	TIME AFTER BOCREC
CORE POWER "ON"	0 SEC.	-105 SEC.
ACC INJ. INITIATION	96	-9
CORE POWER DECAY INITIATION	101	-4
BOCREC	105	0
SWITCH ACC TO LPCI	116	11
MAXIMUM CONT - II PRESSURE (0.425 MPA)	118	13
MAXIMUM ECC INJ. PATE (22 KG/SEC)	119	14
MAXIMUM CORE PRESSURE (0.475 MPA)	120	15
MAXIMUM CORE TEMPERATURE (1000K)	137	32
WHOLE CORE QUENCHED	308	203
MAXIMUM CORE INLET SUBCOOLING (14.7 K)	320	215

Table 5 Chronology of Test S1-01

	TIME AFTER CORE POWER"ON"	TIME AFTER BOCREC
COER POWER "ON"	0 SEC.	-107 SEC.
ACC INJ. INITIATION	97	-10
CORE POWER DECAY INITIATION	102	-5
BOCREC	107	0
SWITCH ACC TO LPCI	117	10
MAXIMUM ECC INJ. RATE (23 KG/SEC)	118	11
MAXIMUM CONT - II PRESSURE (0.218 MPA)	127	20
MAXIMUM CORE TEMPERATURE (1012 K)	140	33
MAXIMUM CORE PRESSURE (0.233 MPA)	155	48
MAXIMUM CORE INLET SUBCOOLING (15.5 K)	160	53
WHOLE CORE QUENCHED	399	292

Table 6 Chronology of Test S1-02

	TIME AFTER CORE POWER"NO"	TIME AFTER BOCREC
CORE POWER "ON"	0 SEC.	-106 SEC.
ACC INJ. INITIATION	95	-11
CORE POWER DECAY INITIATION	100	-6
BOCREC	106	0
SWITCH ACC TO LPCI	115	9
MAXIMUM ECC INJ. RATE (21.7 KG/SEC)	115	9
MAXIMUM CONT - II PRESSURE (0.169 MPA)	124	18
MAXIMUM CORE TEMPERATURE (1016 K)	153	47
MAXIMUM CORE PRESSURE (0.214 MPA)	173	67
MAXIMUM CORE INLET SUBCOOLING (19.0 K)	173	67
WHOLE CORE QUENCHED	452	346

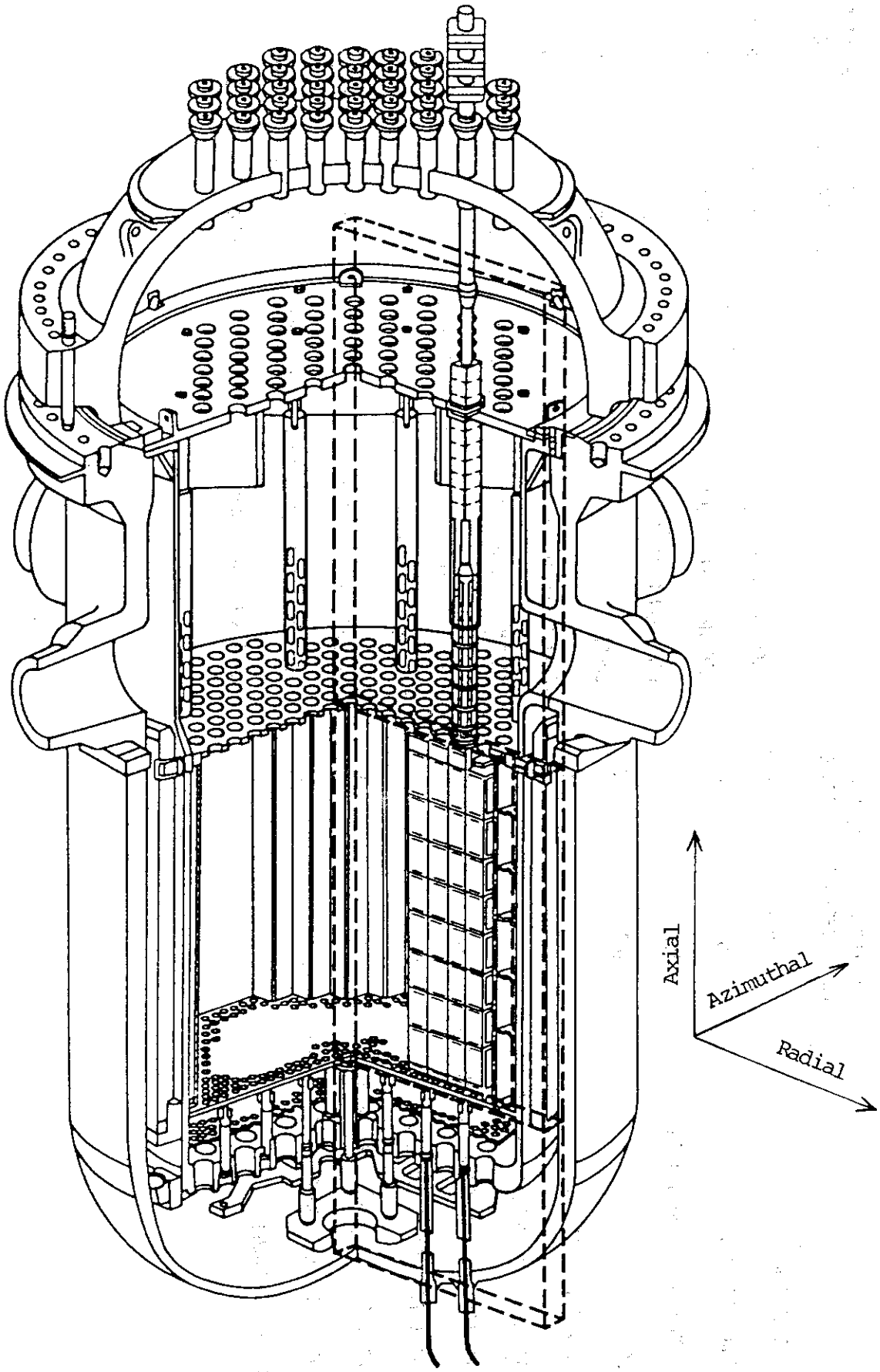

Fig. 1 Simulated Part of a PWR with Slab Core Test Facility (SCTF)

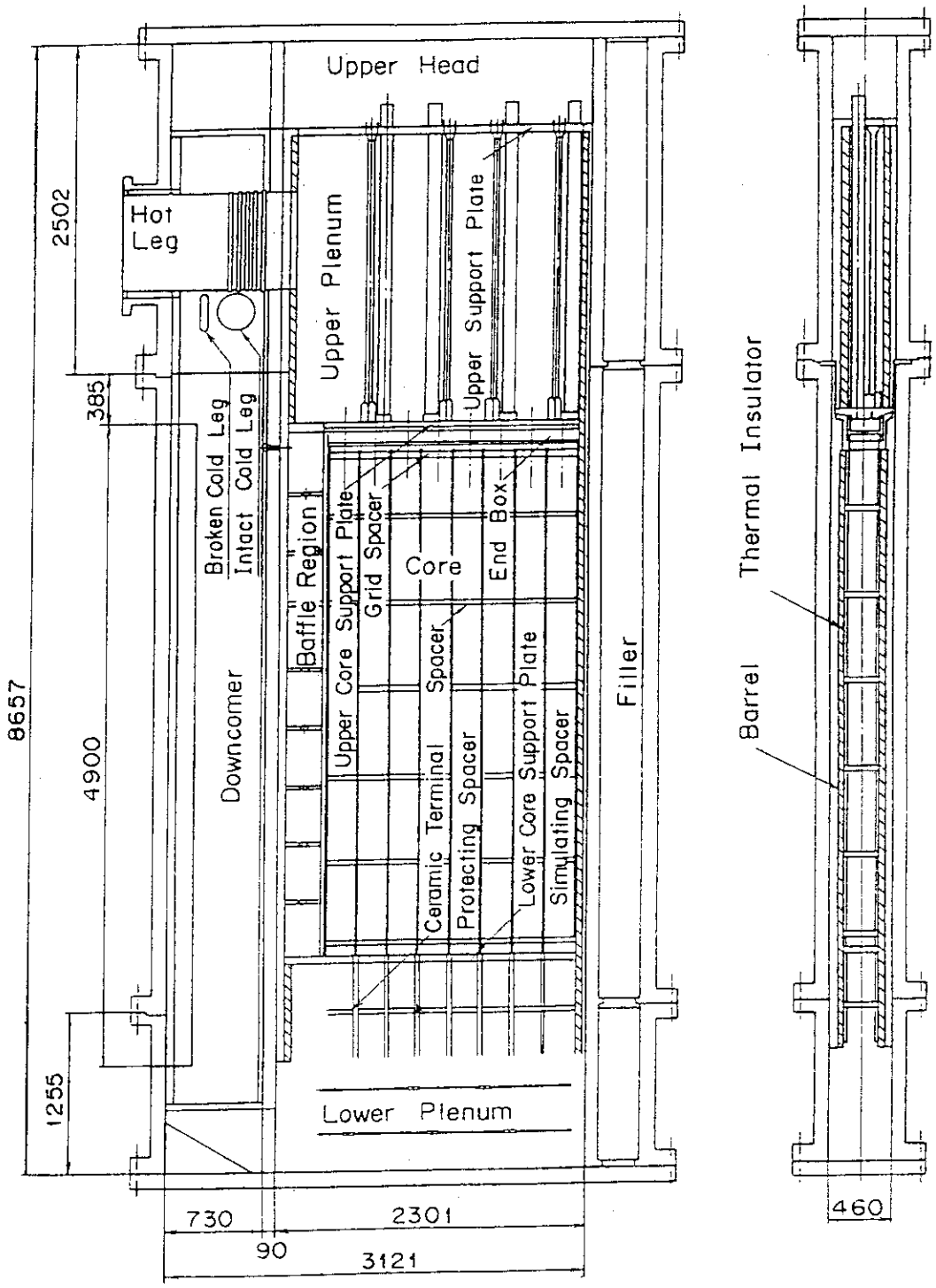

Fig. 2 Vertical Cross Section of the Pressure Vessel

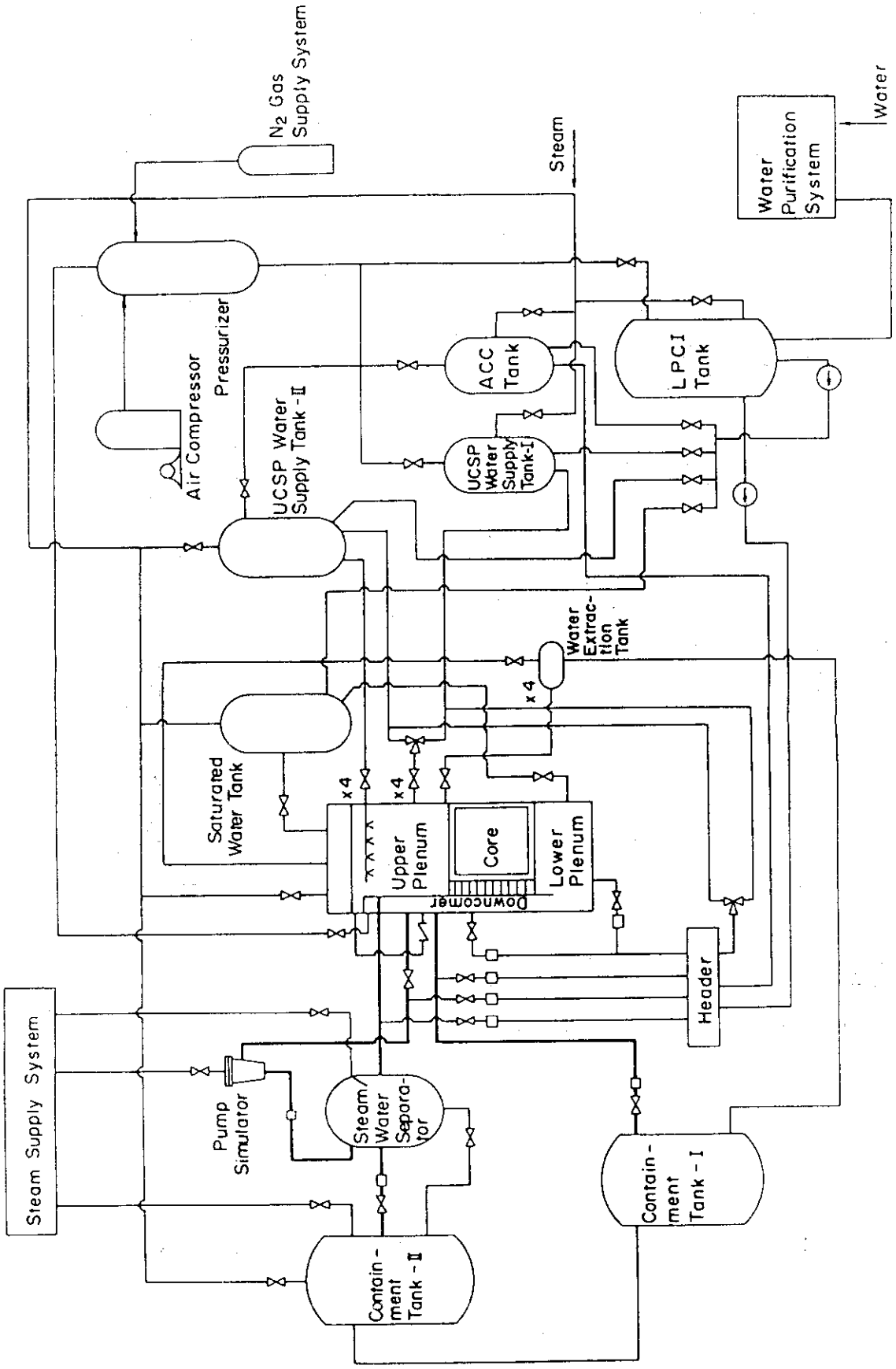

Fig. 3 Flow Sheet of Slab Core Test Facility

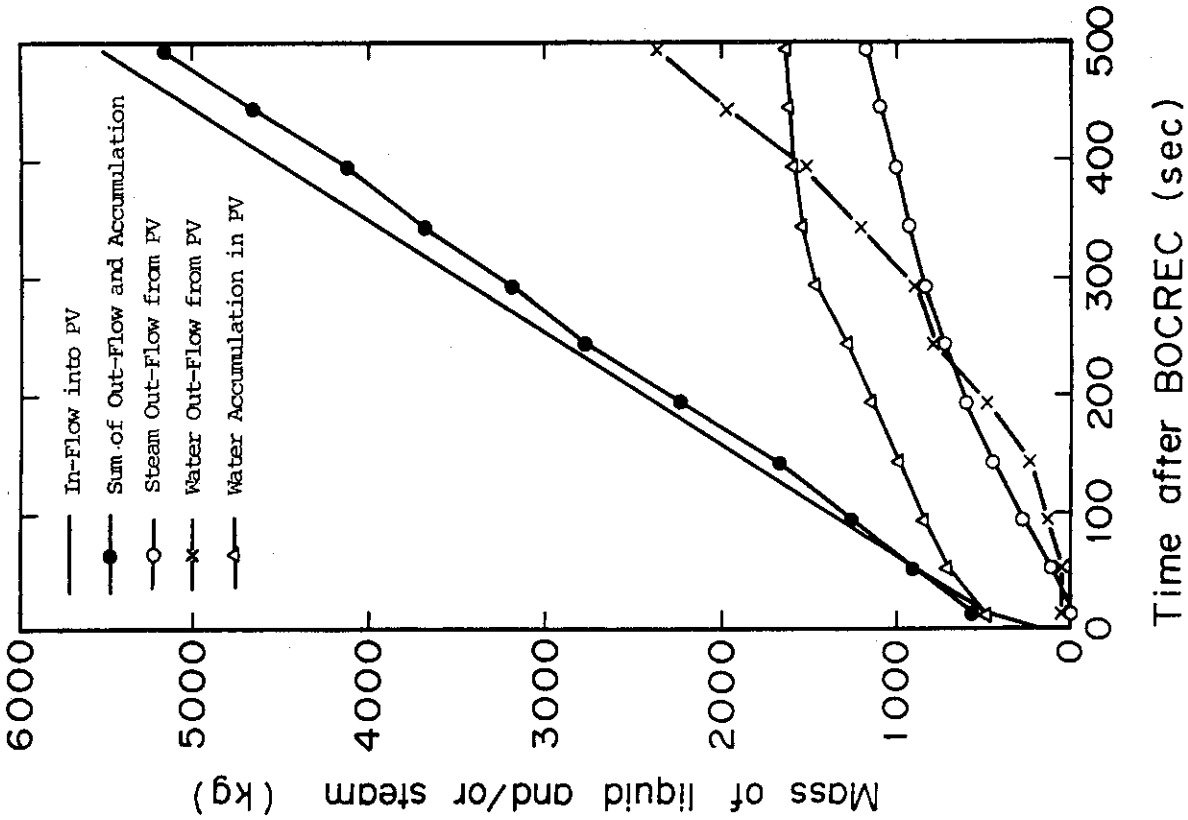

Fig. 5 Mass Balance in the Pressure Vessel in Test S1-01

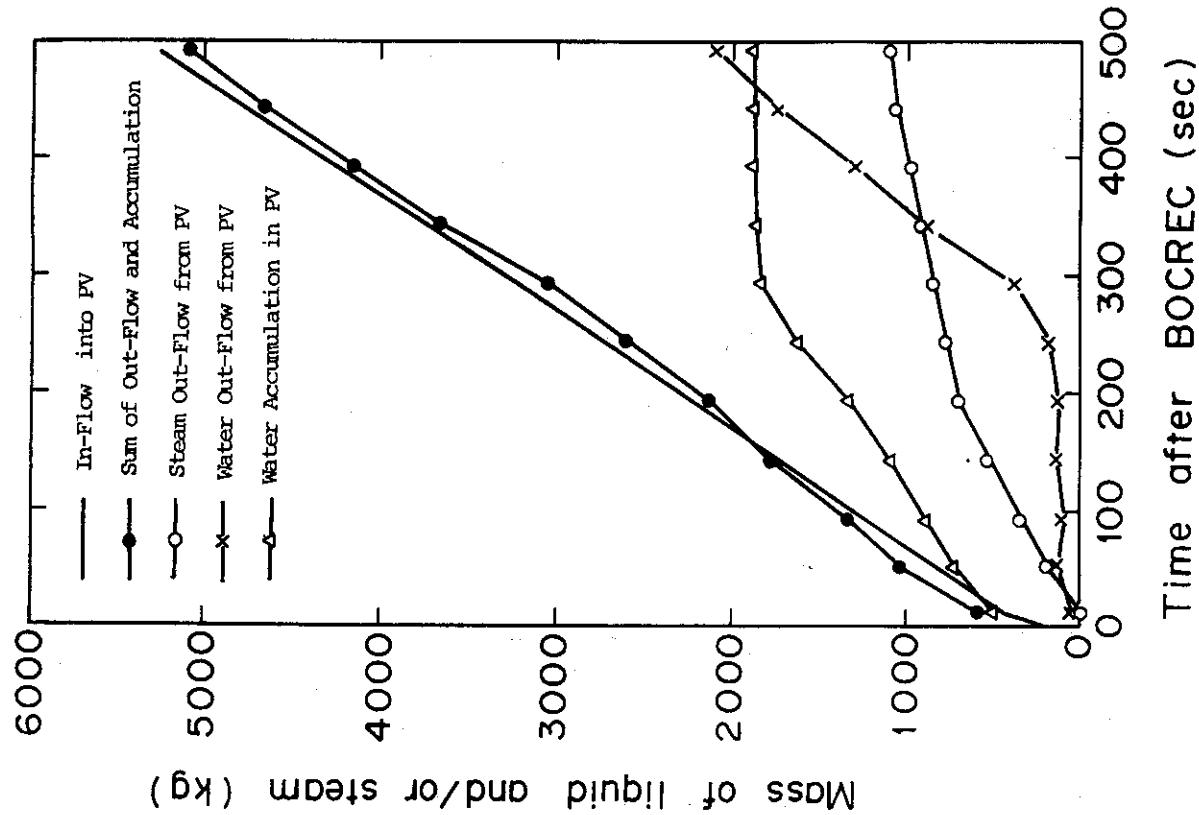

Fig. 4 Mass Balance in the Pressure Vessel in Test S1-SH2

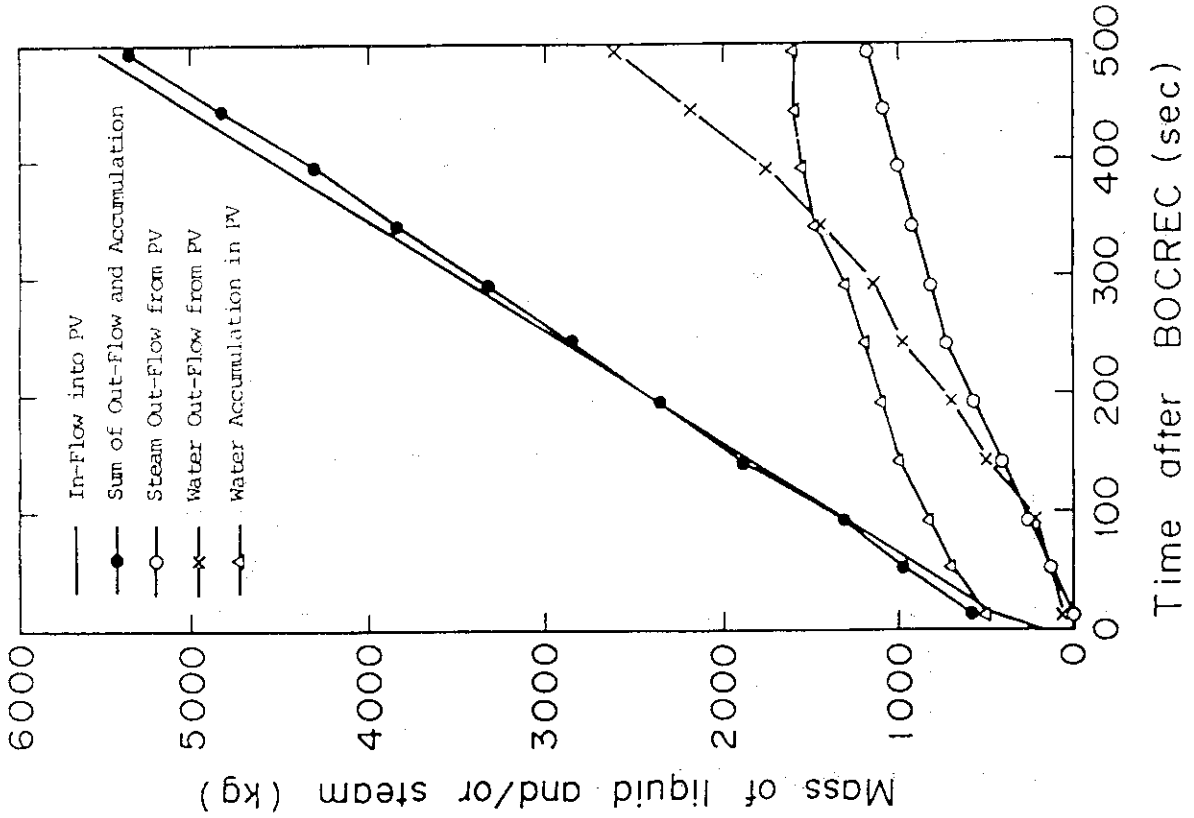

Fig. 6 Mass Balance in the Pressure Vessel in Test S1-02

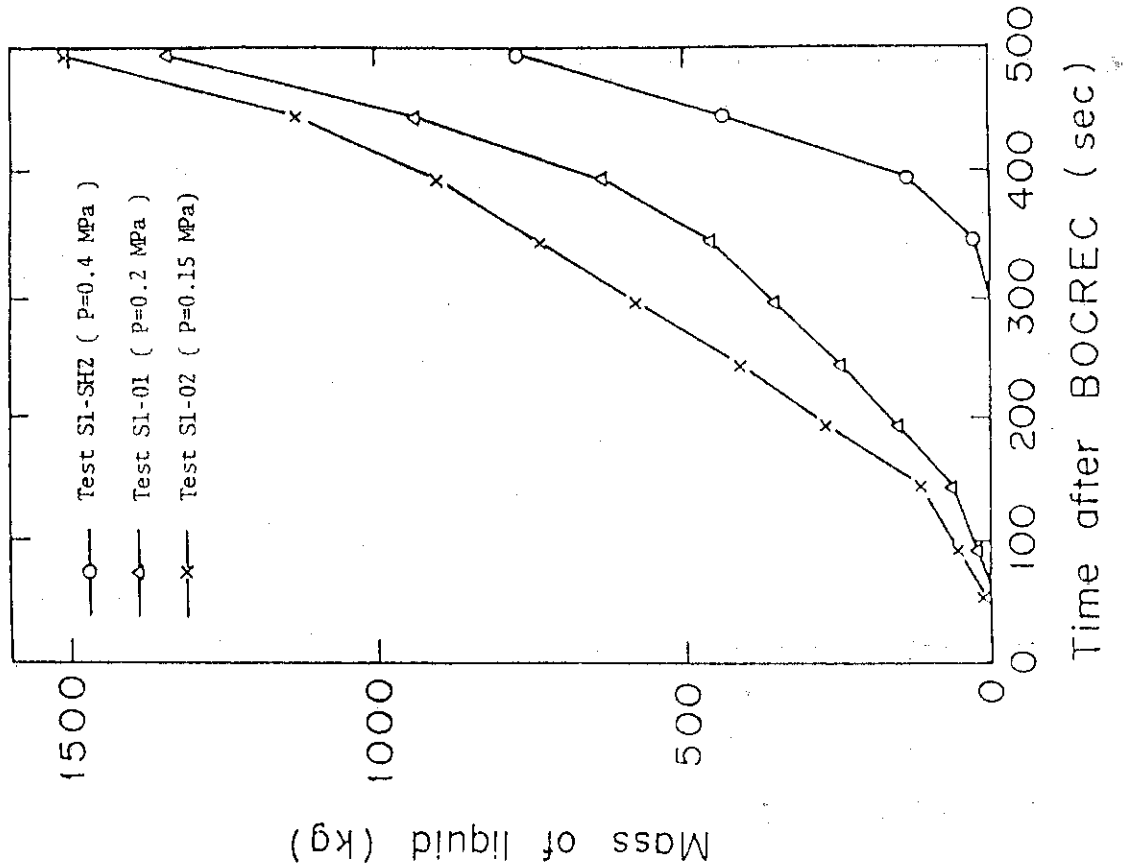

Fig. 7 Integration of Carryover Water through Hot Leg

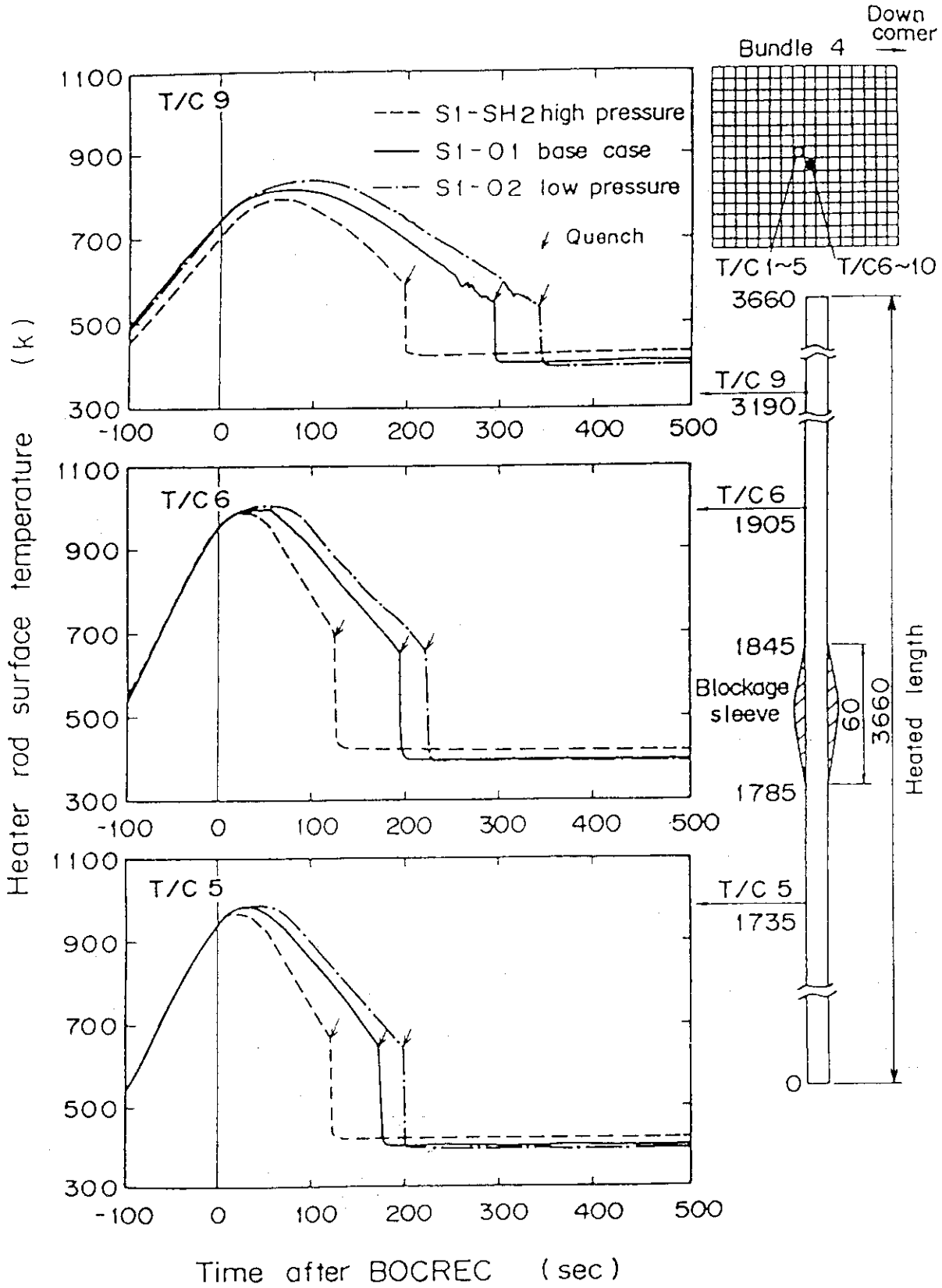

Fig. 8 Typical Cladding Temperature Histories

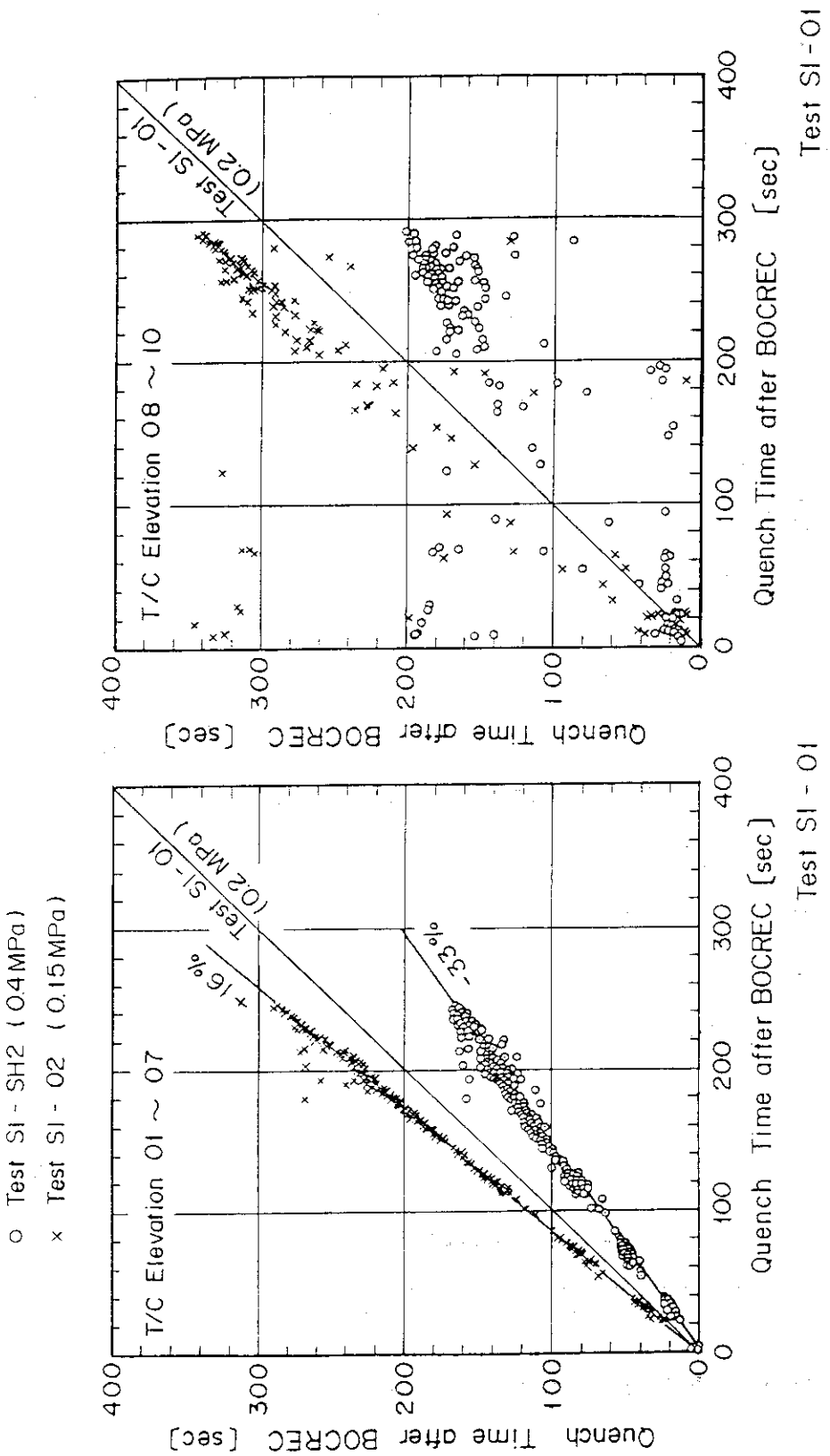

(a) Middle and Lower Part of the Core Test SI - 01

(b) Upper Part of the Core Test SI - 01

Fig. 9 Comparison of Quench Time among the Three System Pressure Effect Tests

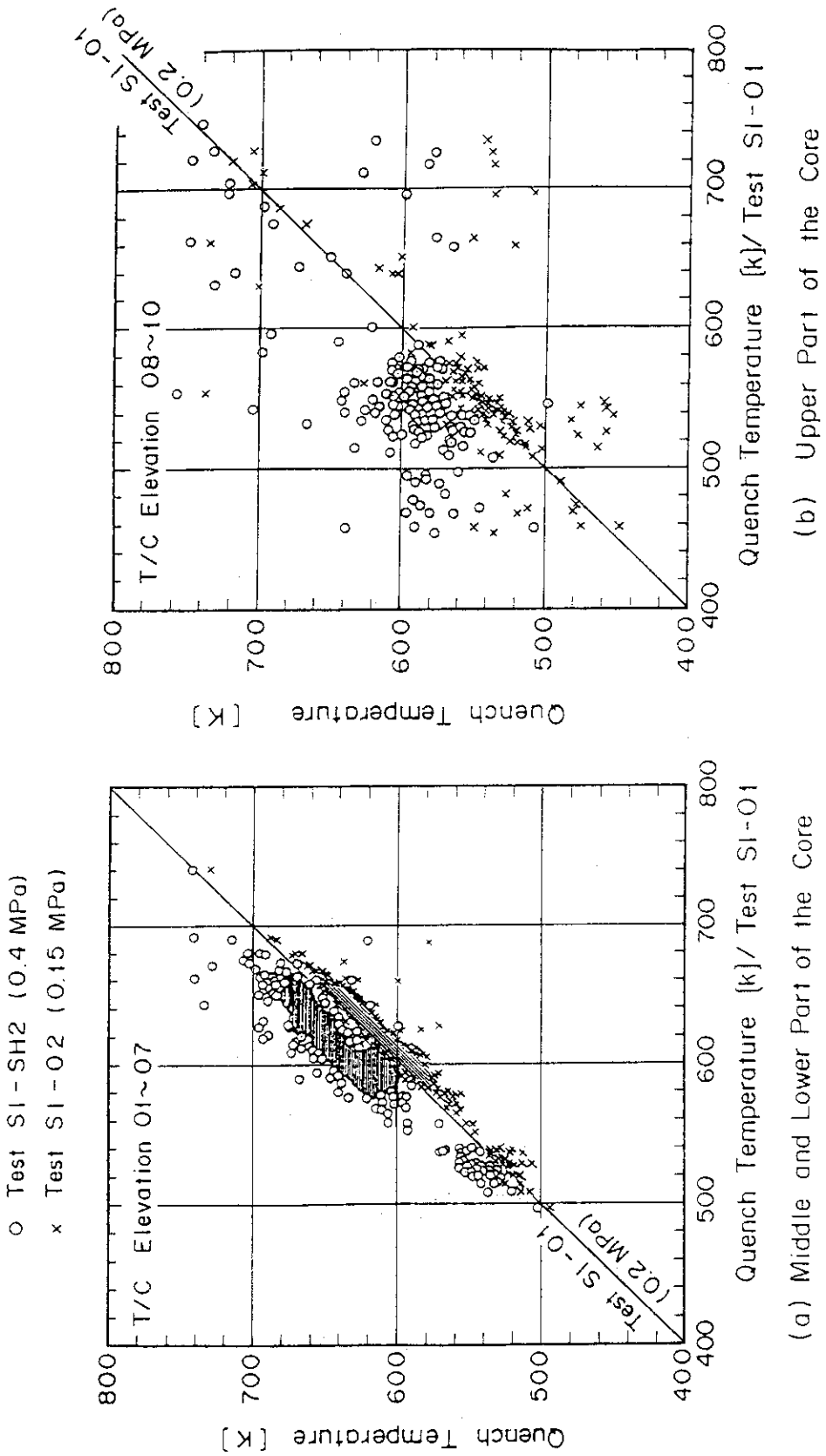

(a) Middle and Lower Part of the Core

(b) Upper Part of the Core

Fig. 10 Comparison of Quench Temperature among the Three System Pressure Effect Tests

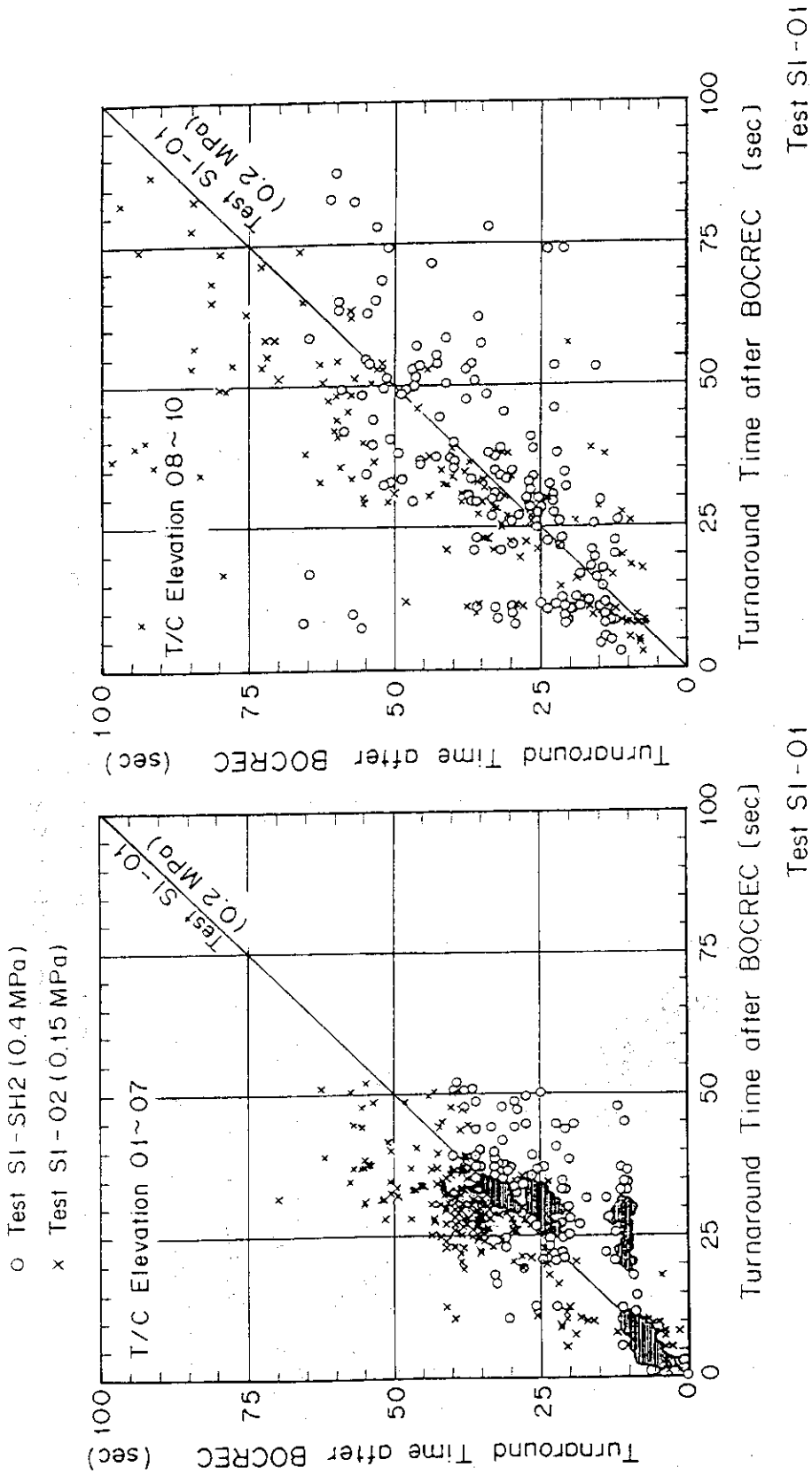

(a) Middle and Lower Part of the Core

(b) Upper Part of the Core

Fig. 11 Comparison of Turnaround Time among the Three System Pressure Effect Tests

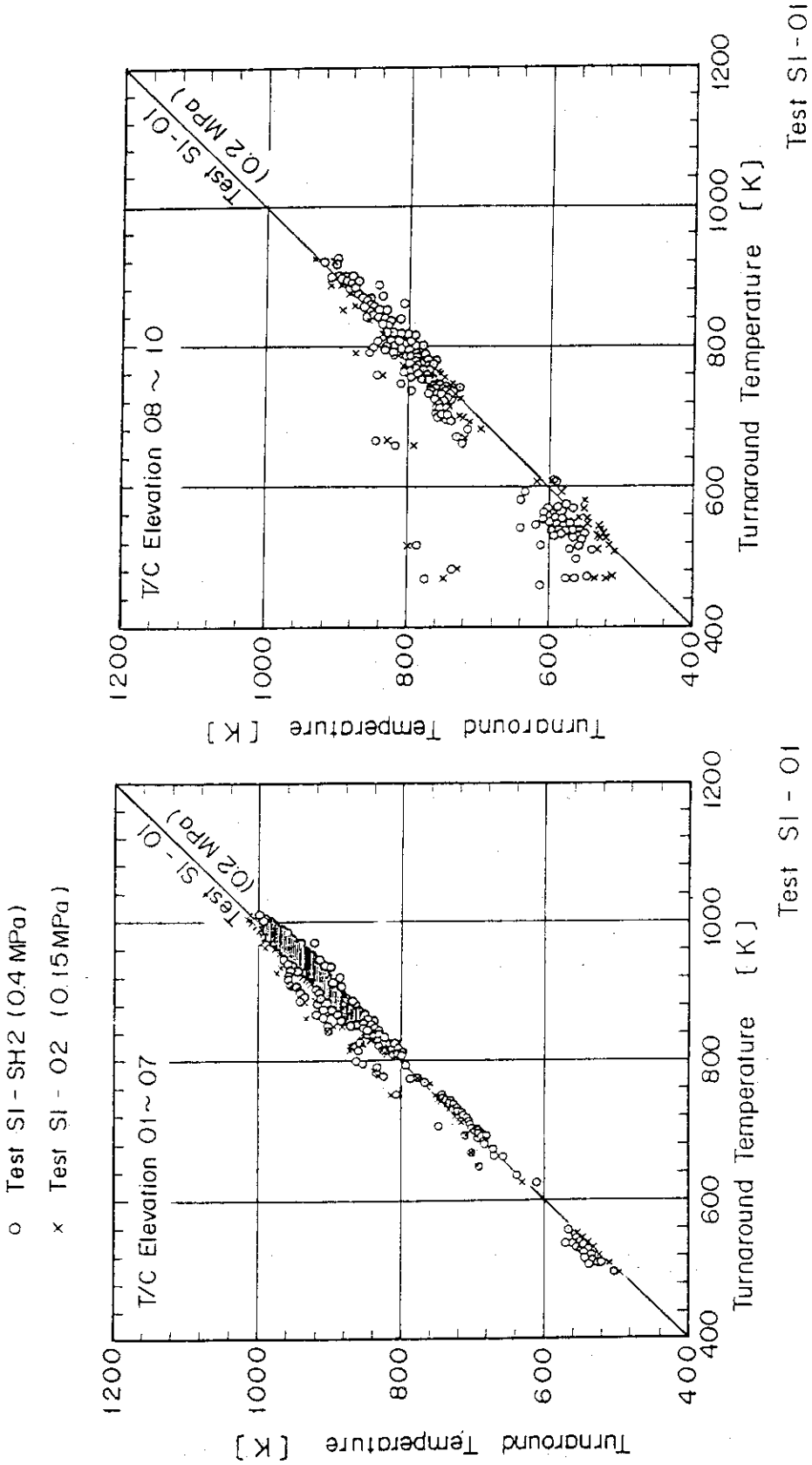

(a) Middle and Lower Part of the Core

(b) Upper Part of the Core

Fig. 12 Comparison of Turnaround Temperature among the Three System Pressure Effect Tests

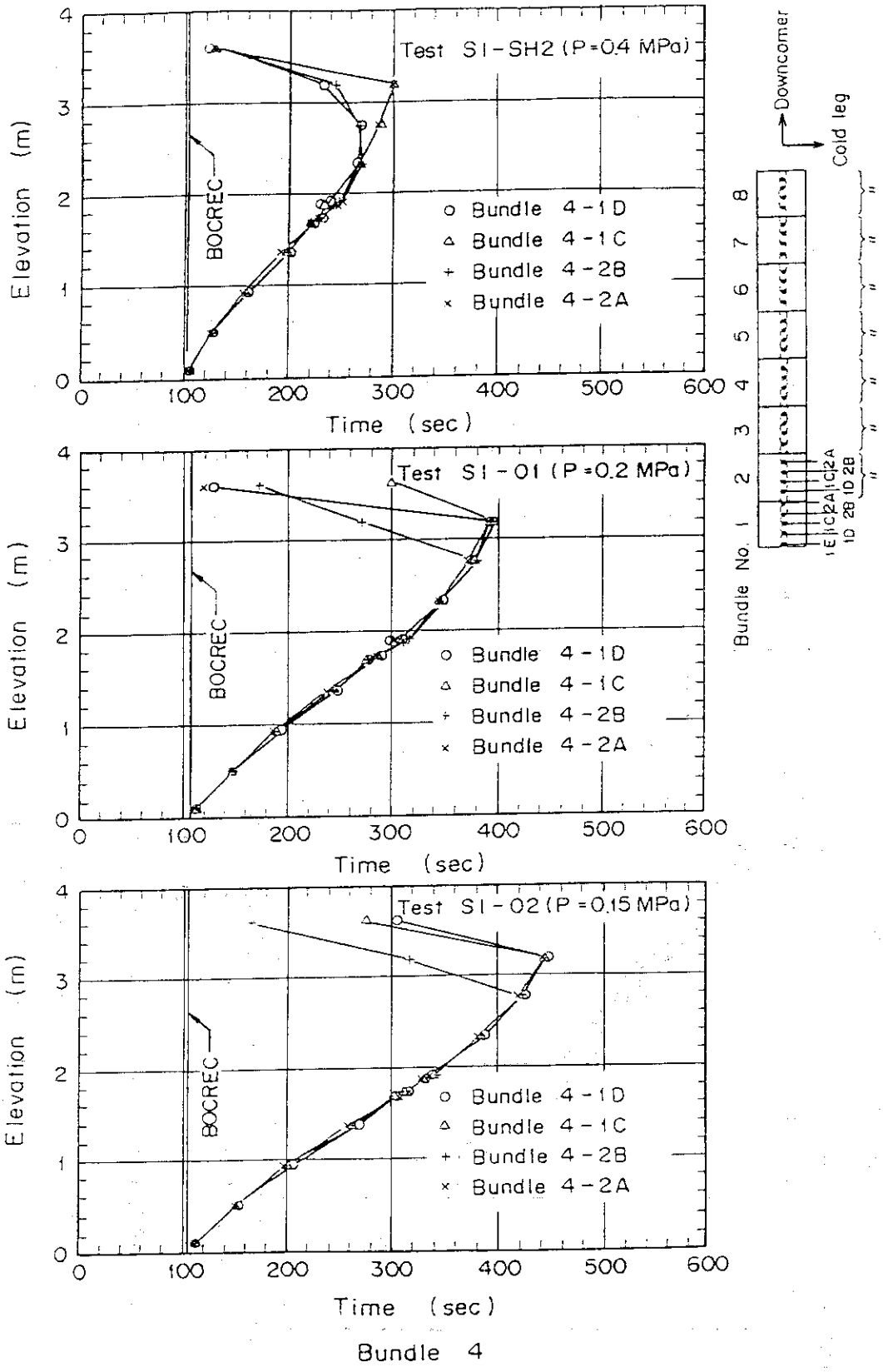

Fig. 13 Typical Quench Envelope for a Blocked Bundle

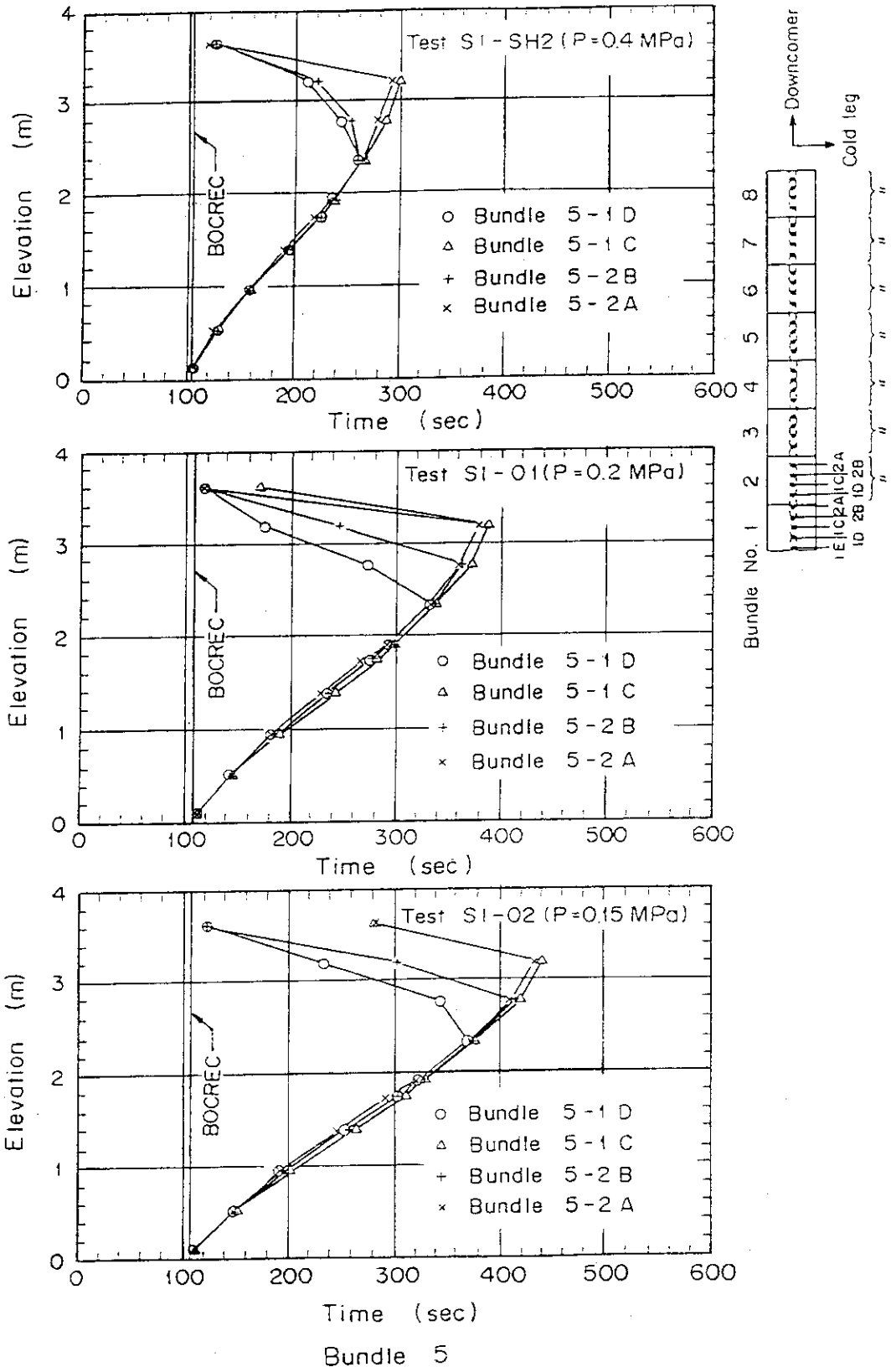

Fig. 14 Typical Quench Envelope for an Unblocked Bundle

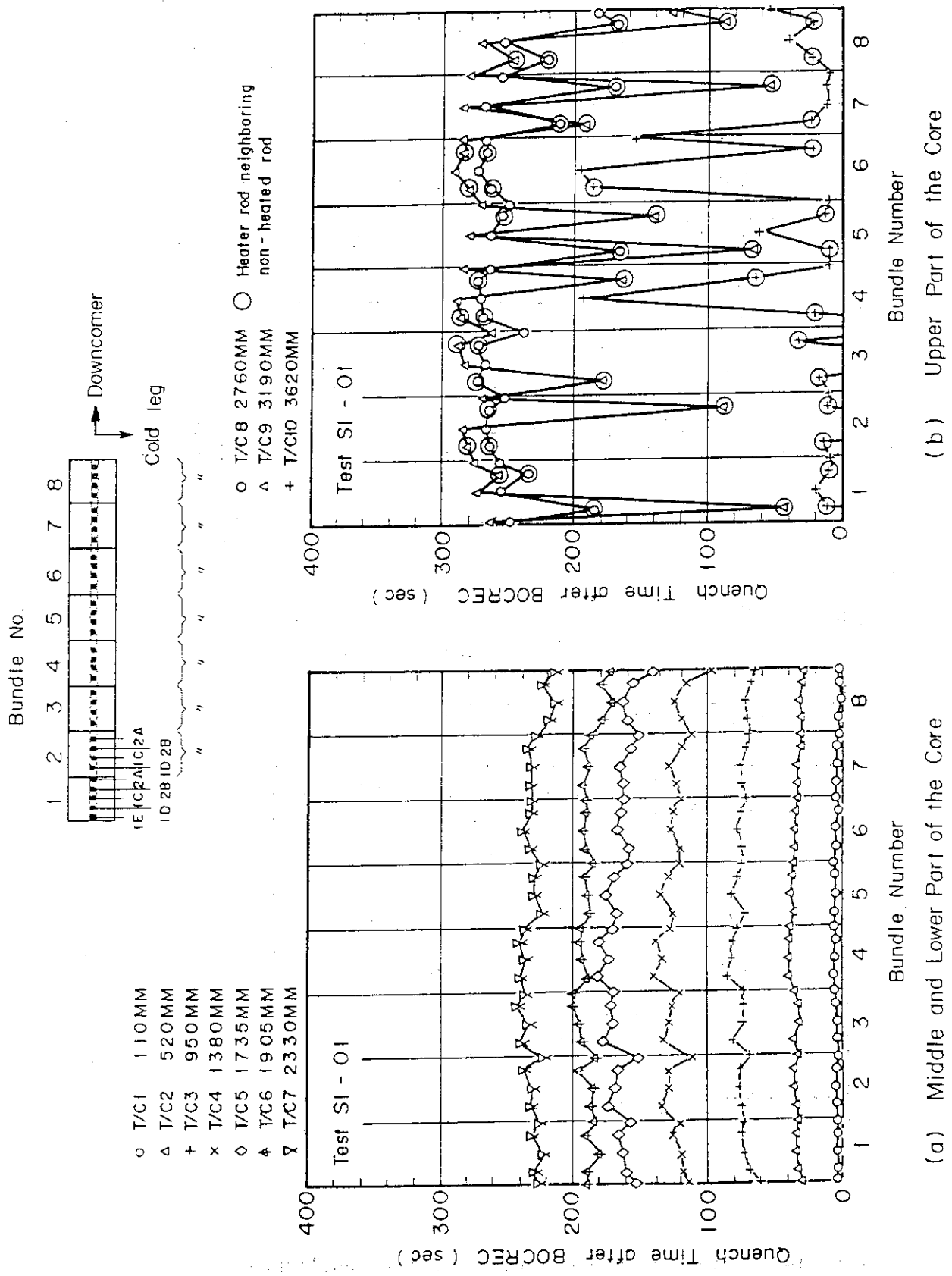

(a) Middle and Lower Part of the Core

(b) Upper Part of the Core

Fig. 15 Radial Distribution of Quench Time

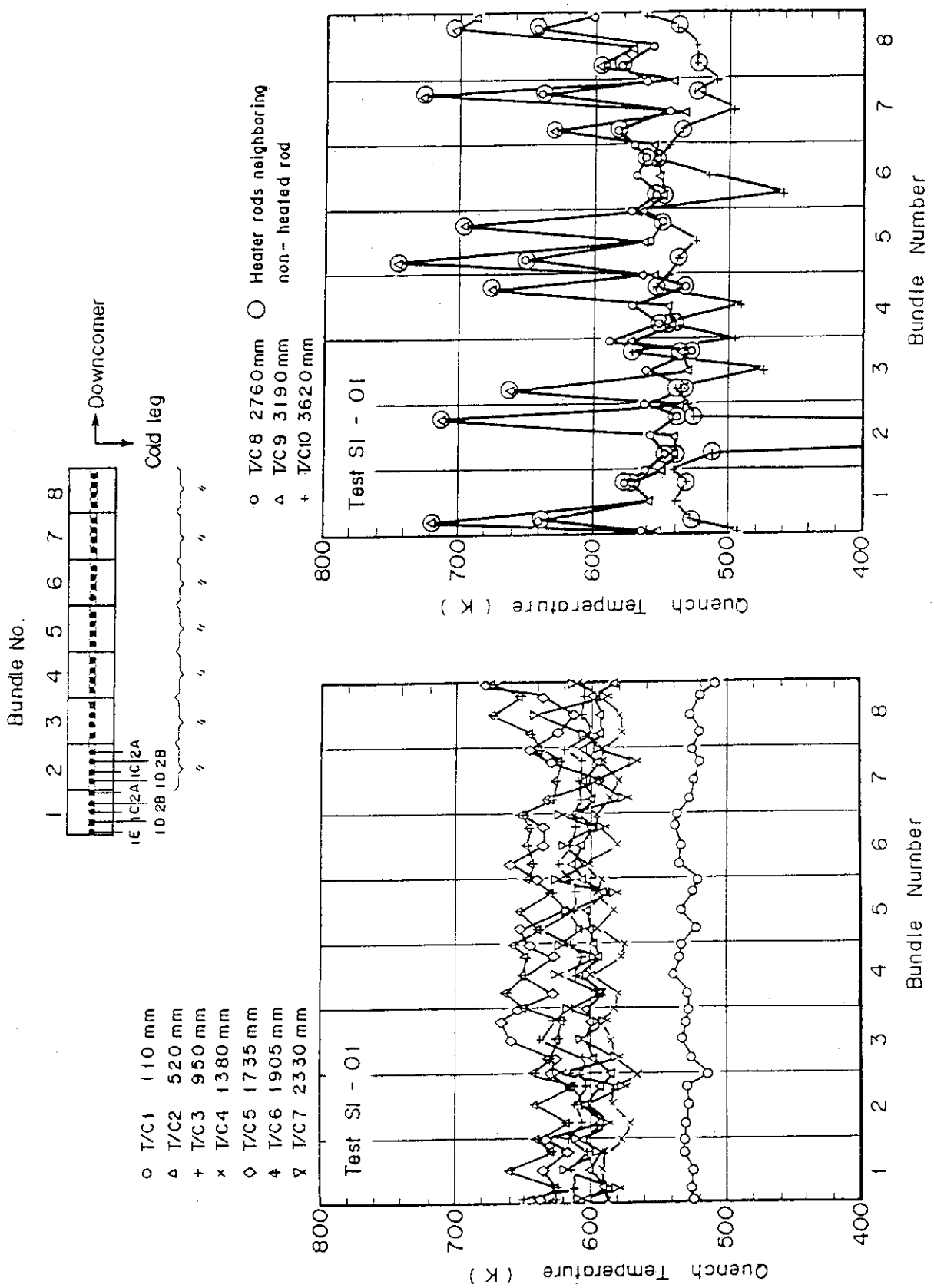

(a) Middle and Lower Part of the Core

(b) Upper Part of the Core

Fig. 16 Radial Distribution of Quench Temperature

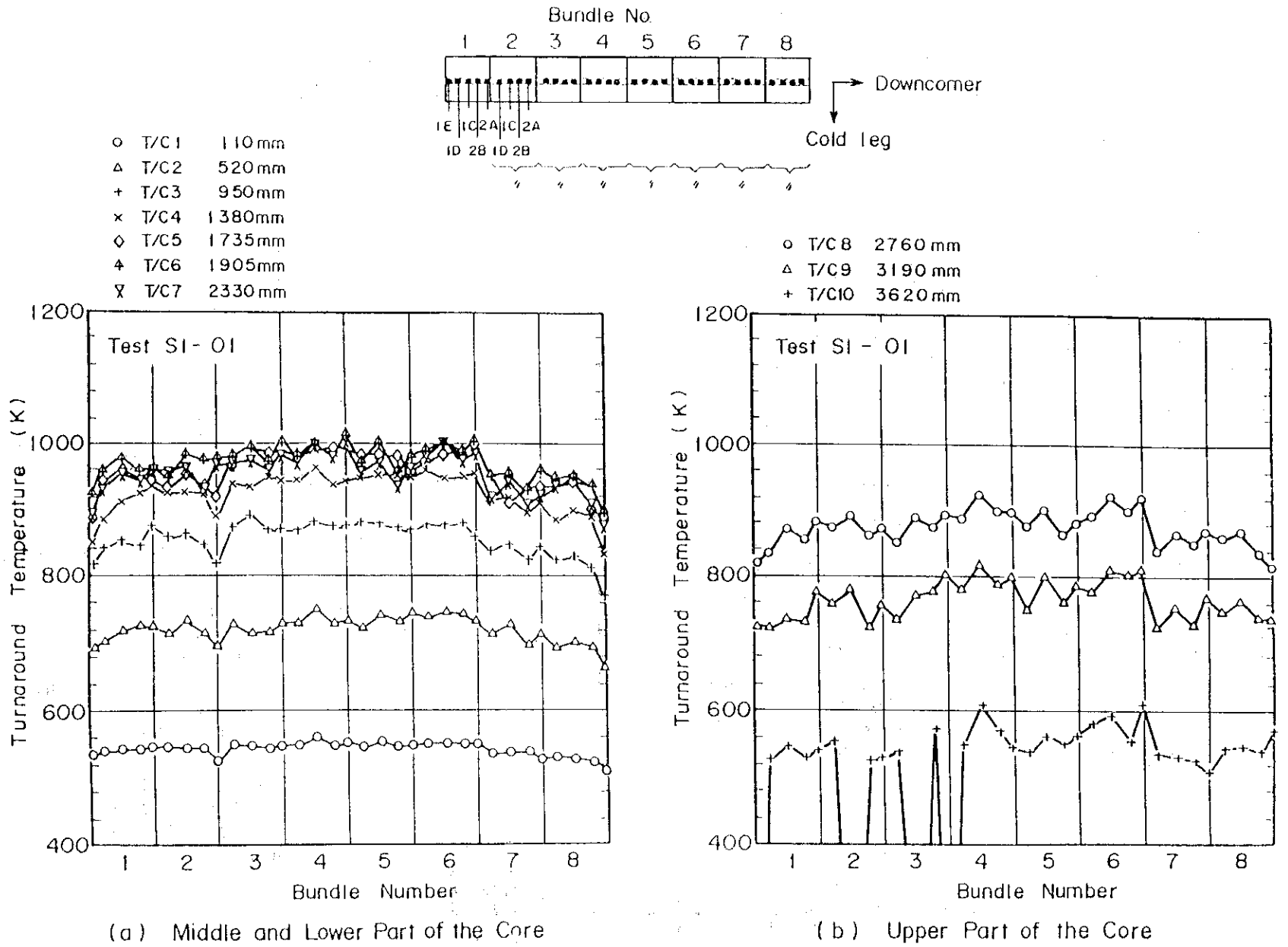

(a) Middle and Lower Part of the Core

(b) Upper Part of the Core

Fig. 17 Radial Distribution of Turnaround Temperature

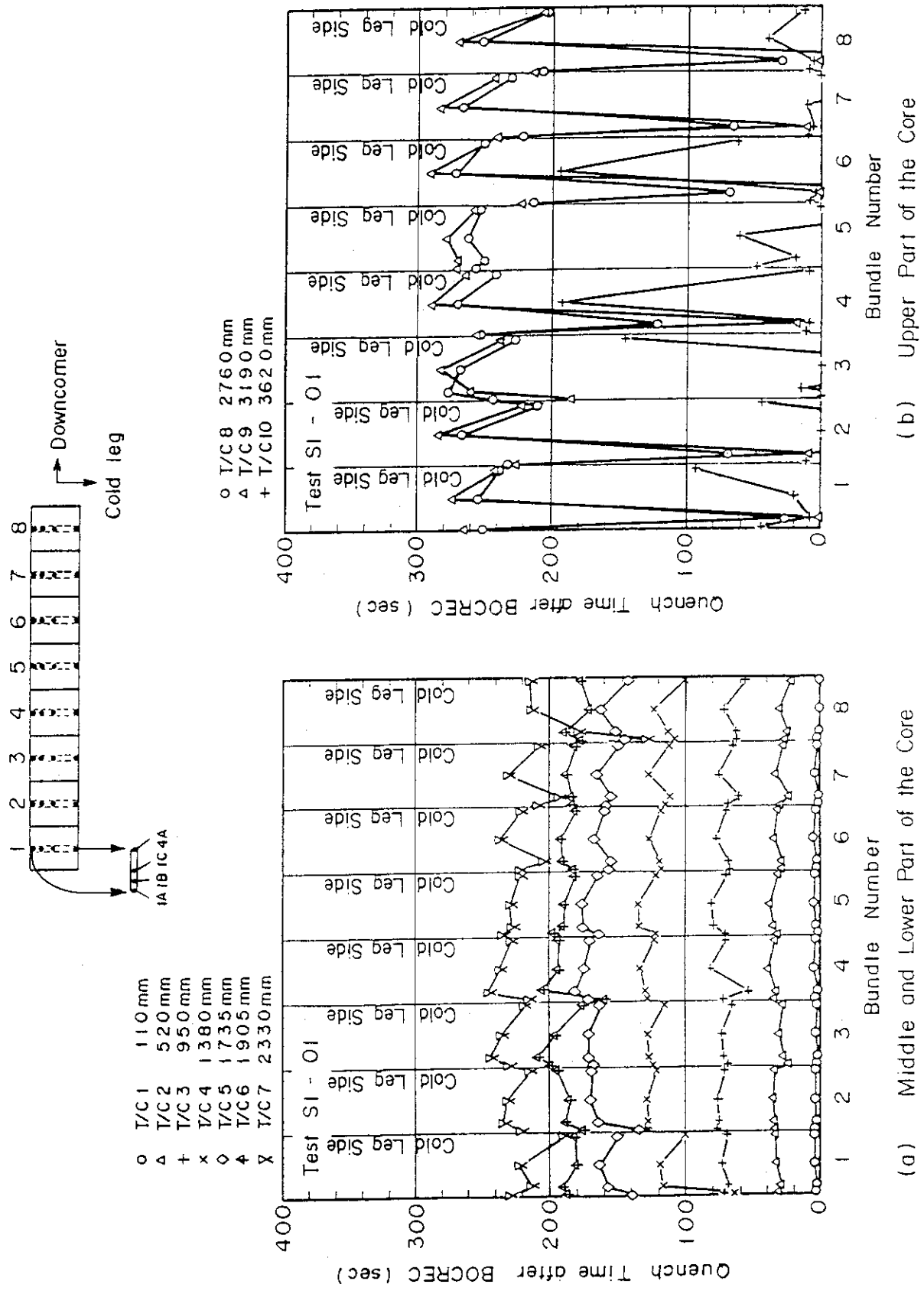

Fig. 18 Azimuthal Distribution of Quench Time

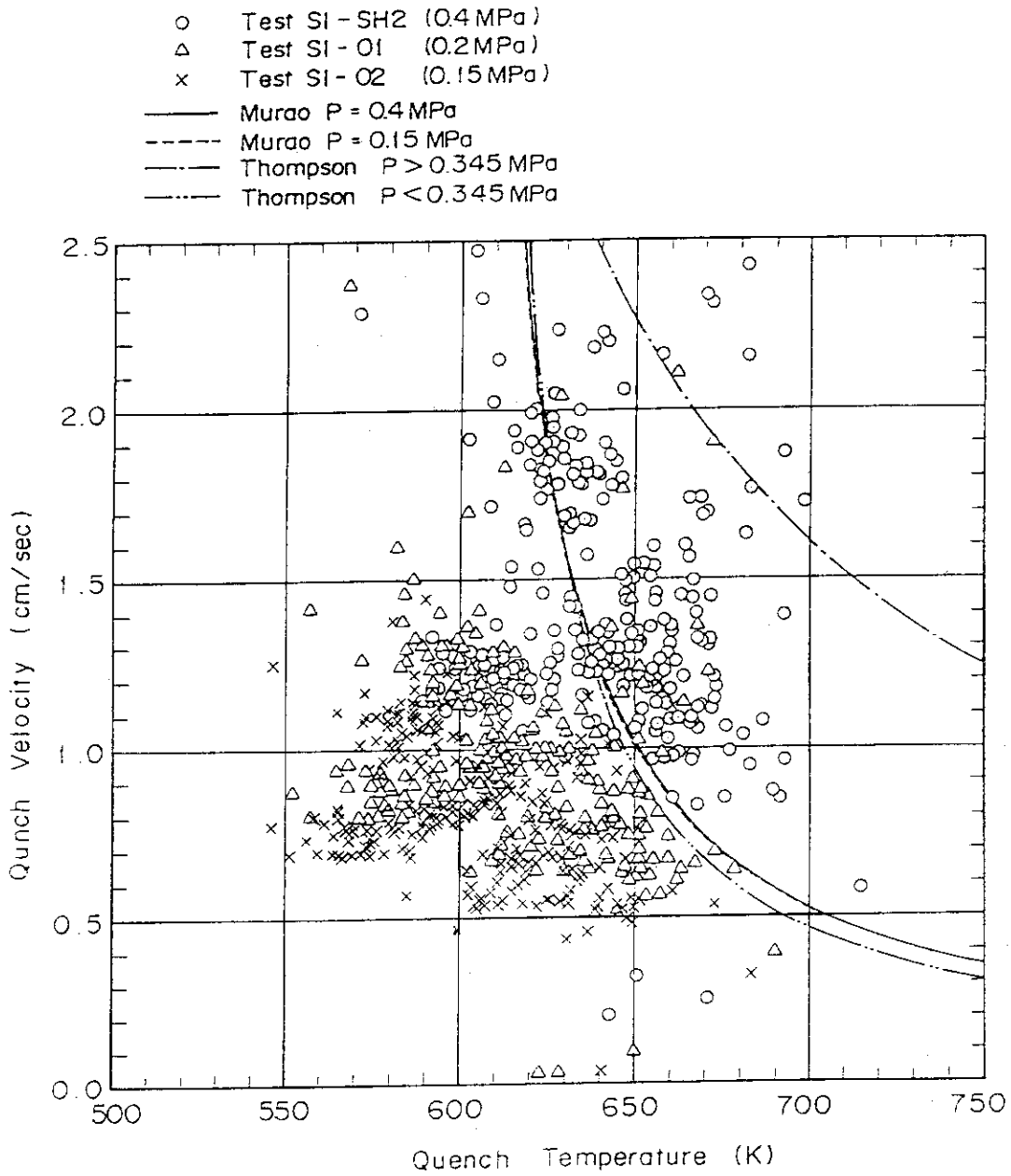

Fig. 19 Comparison of Quench Velocity Data with Murao's and Thompson's Correlations

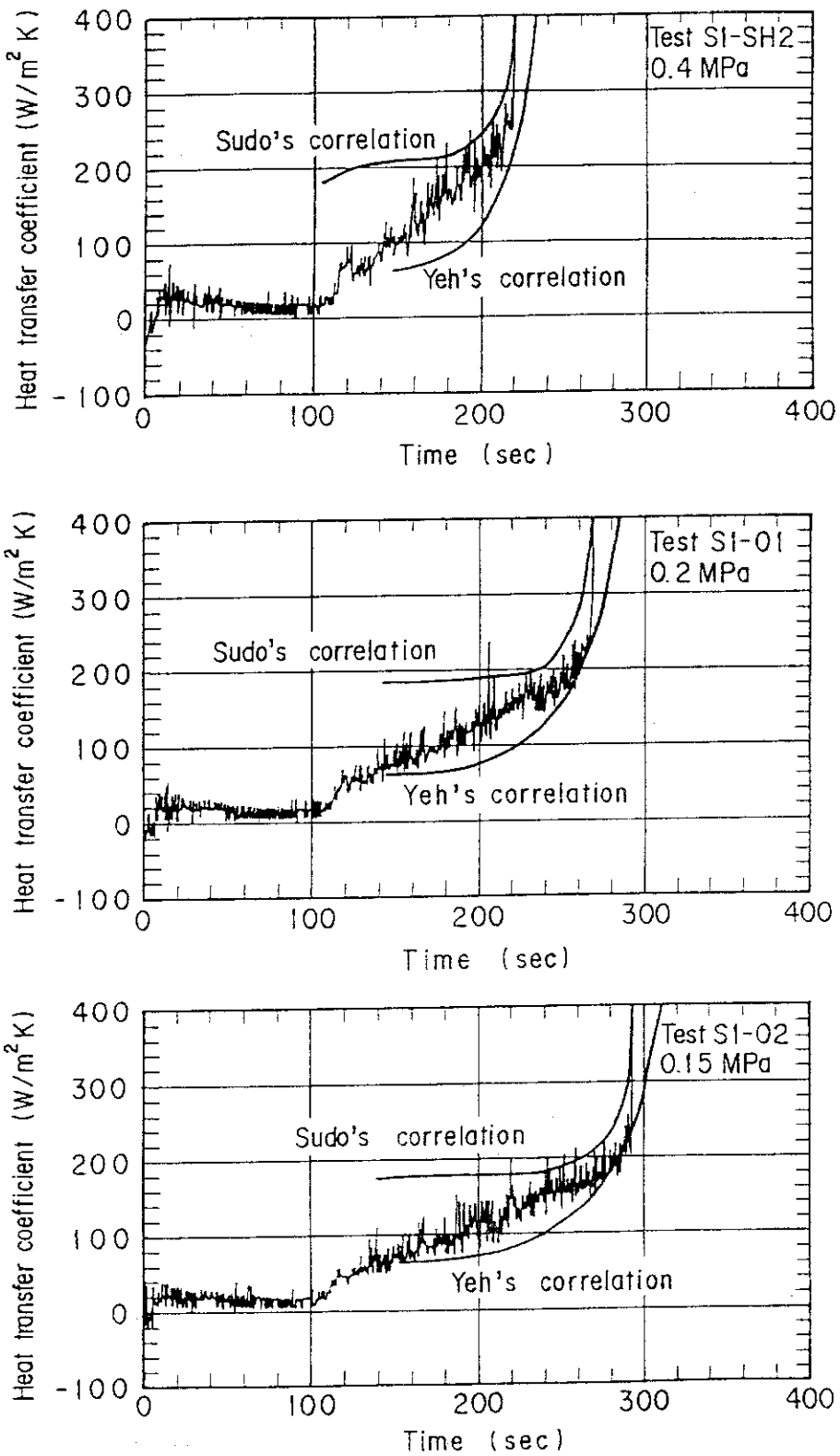

Fig. 20 Change of Core Heat Transfer Coefficient at T/C Elecation 5 of Bundle No.1 in Tests S1-SH2(0.4MPa), S1-01(0.2MPa) and S1-02(0.15MPa)

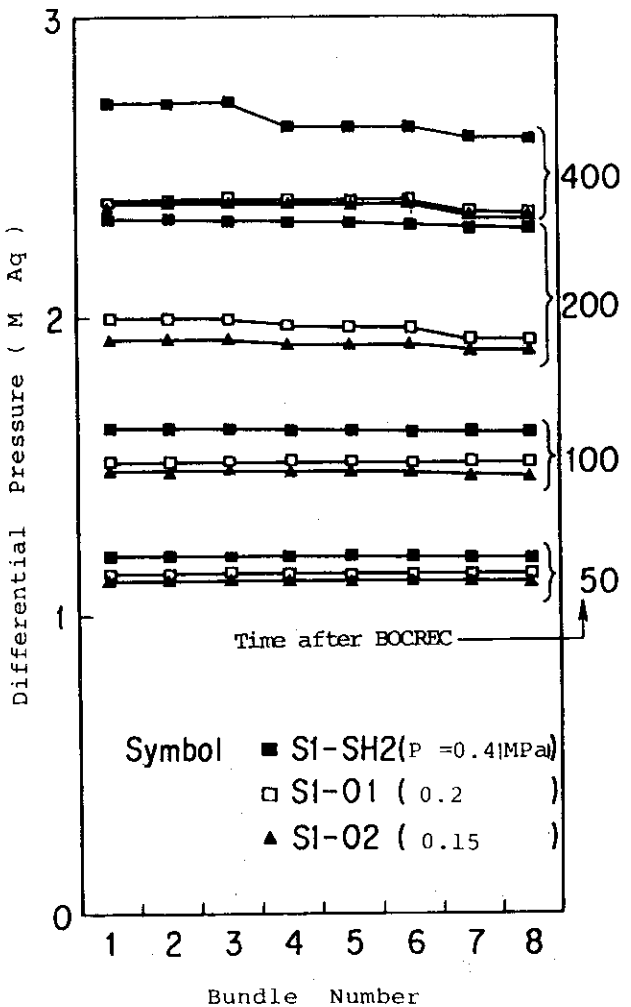

Fig. 21 Horizontal Distribution of Differential Pressure across Core Full Height for Three Different System Pressures

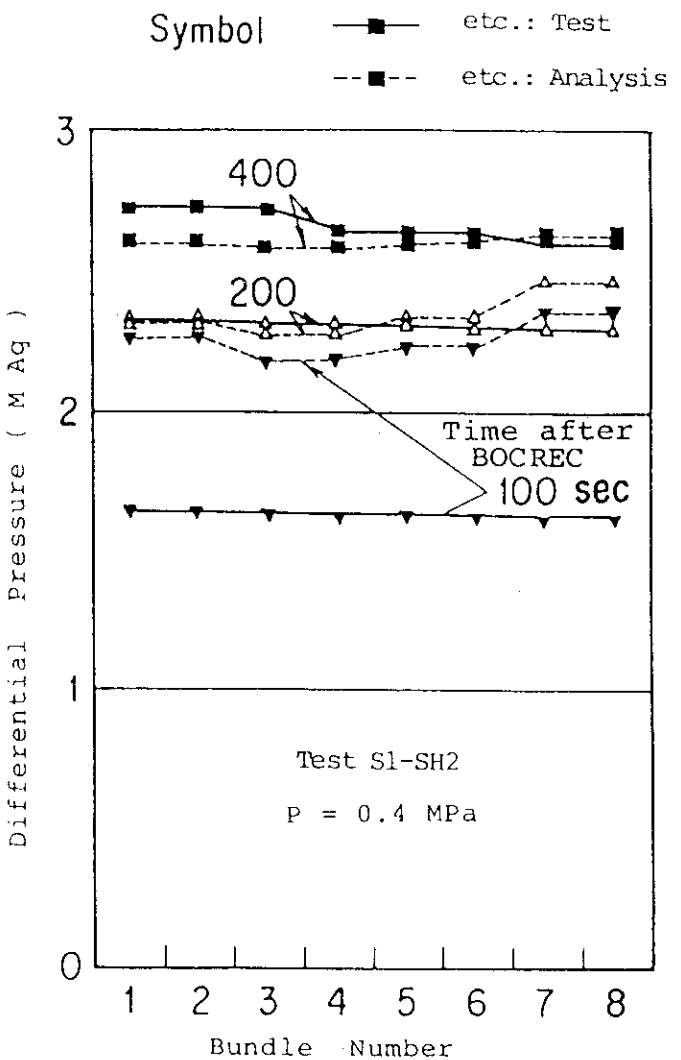

Fig. 22 Comparison of Horizontal Distribution of Differential Pressure across Core Full Height between the Test Results and the Prediction Based on One-Dimensional Analysis

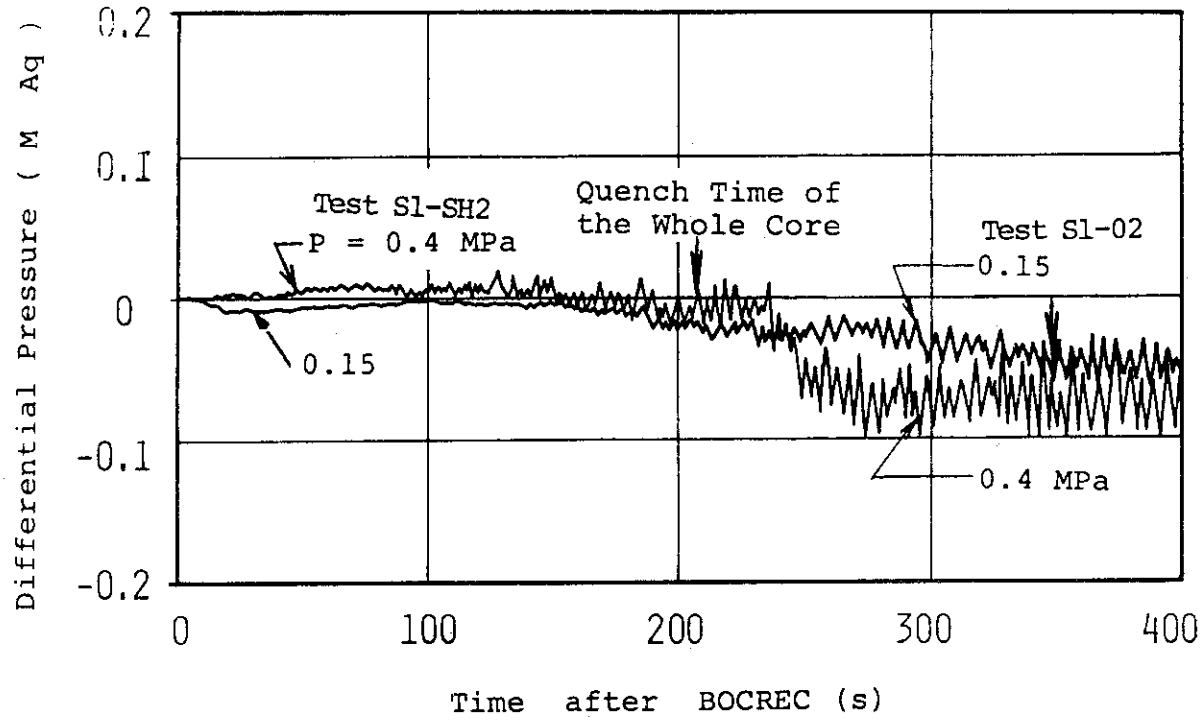

Fig. 23 Horizontal Differential Pressure at Elevation 1905 mm above the Bottom of Heated Part of Rods between Bundle No. 1 and Bundle No. 8(Positive sign shows the pressure at bundle No. 1 is higher than that at bundle No. 8)

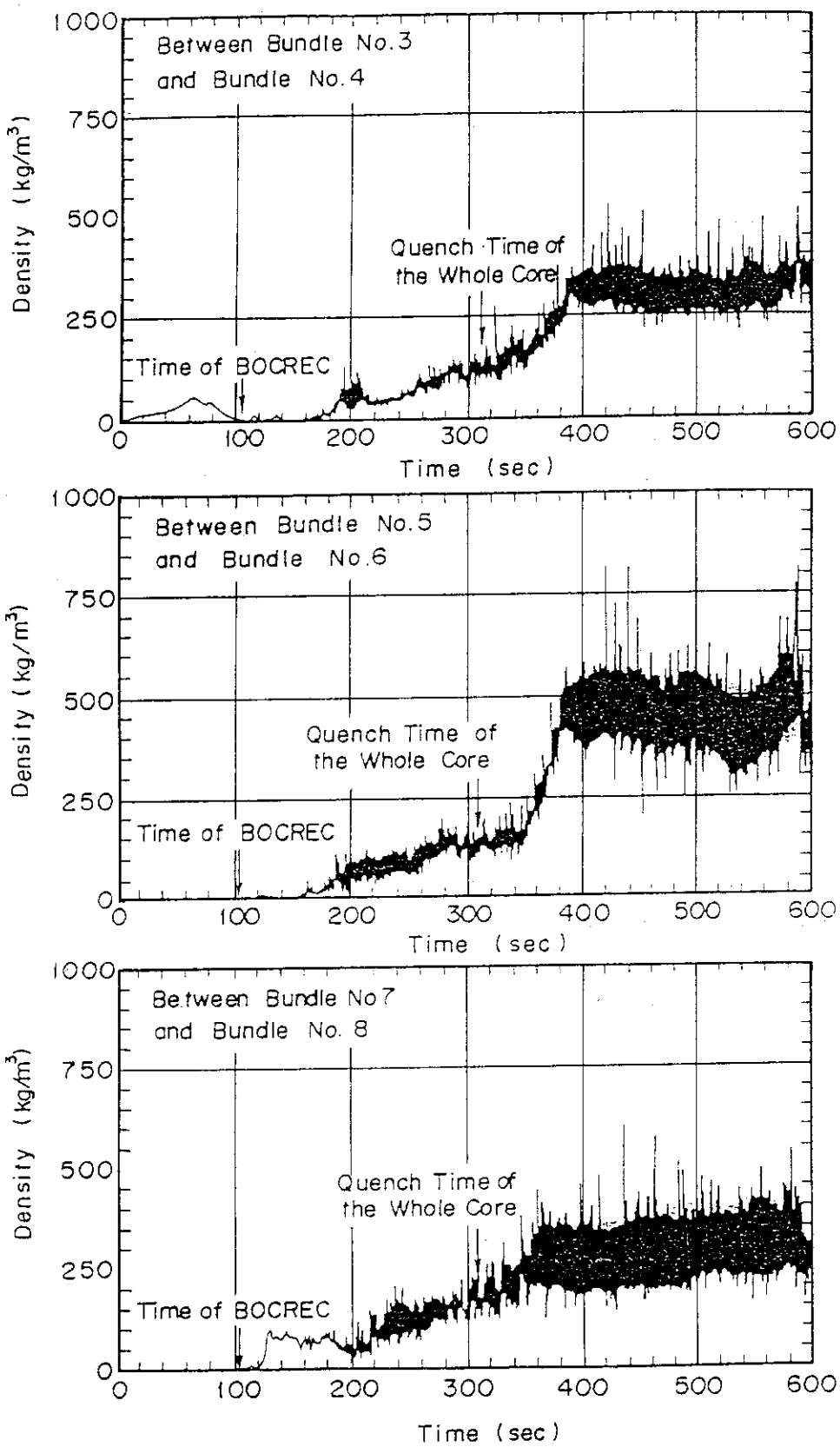

Fig. 24 Transients of Fluid Density at Elevation 2570 mm above the Bottom of Heated Part of Rods in Test S1-SH2 (P=0.4MPa)

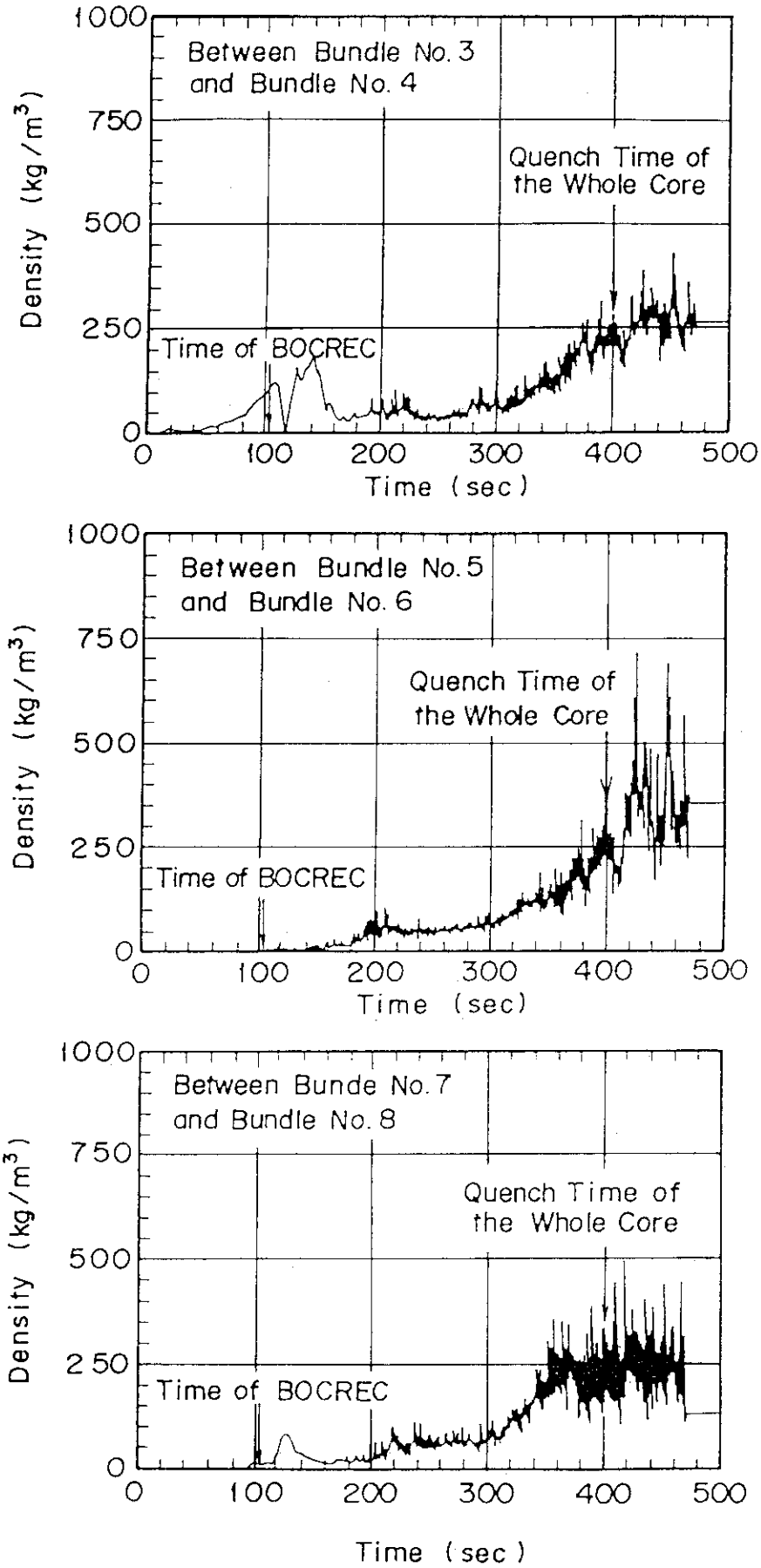

Fig. 25 Transients of Fluid Density at Elevation 2570 mm above the Bottom of Heated Part of Rods in Test S1-01(P=0.2MPa)

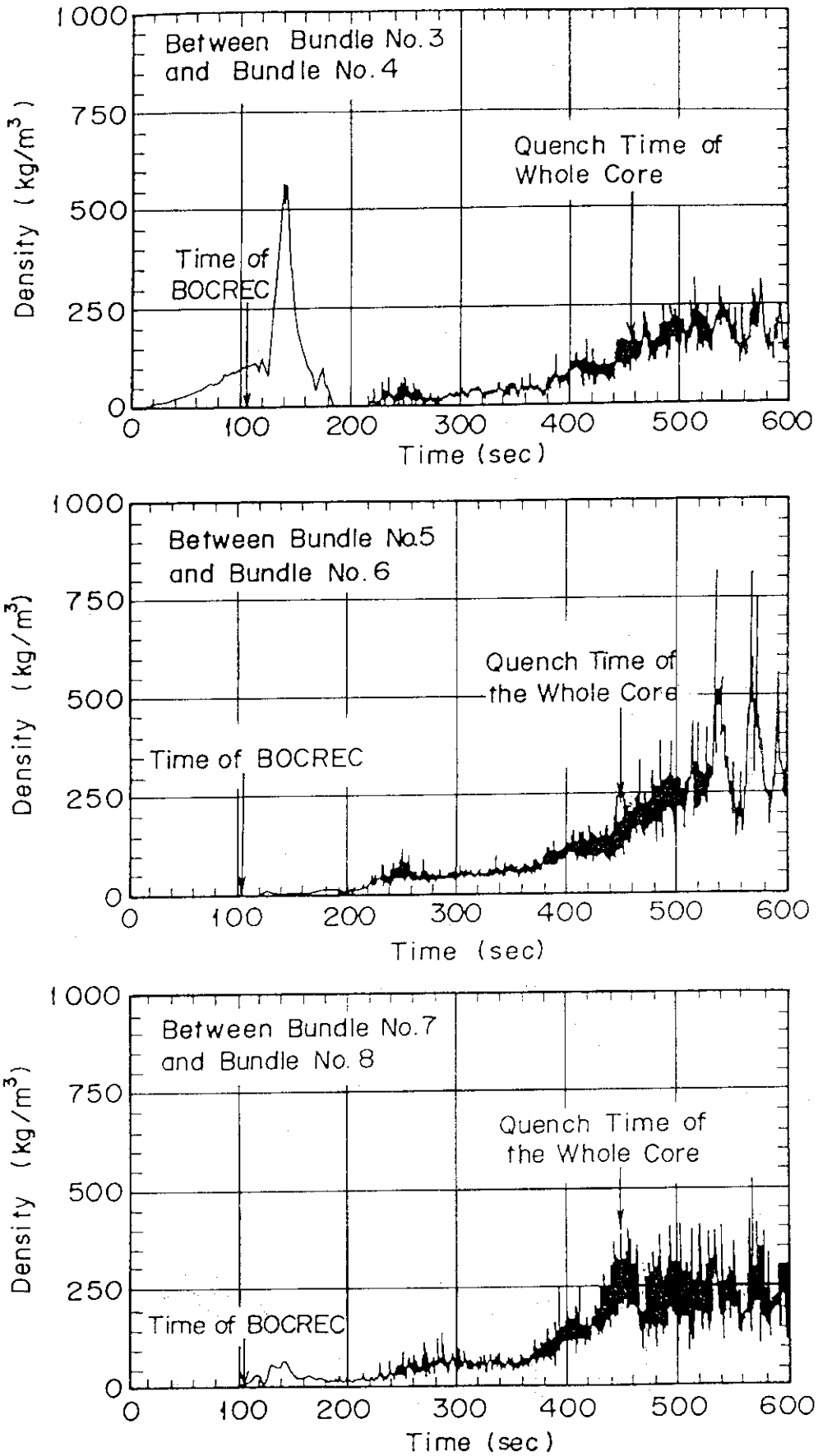

Fig. 26 Transients of Fluid Density at Elevation 2570 mm above the Bottom of Heated Part of Rods in Test S1-02(P=0.15MPa)

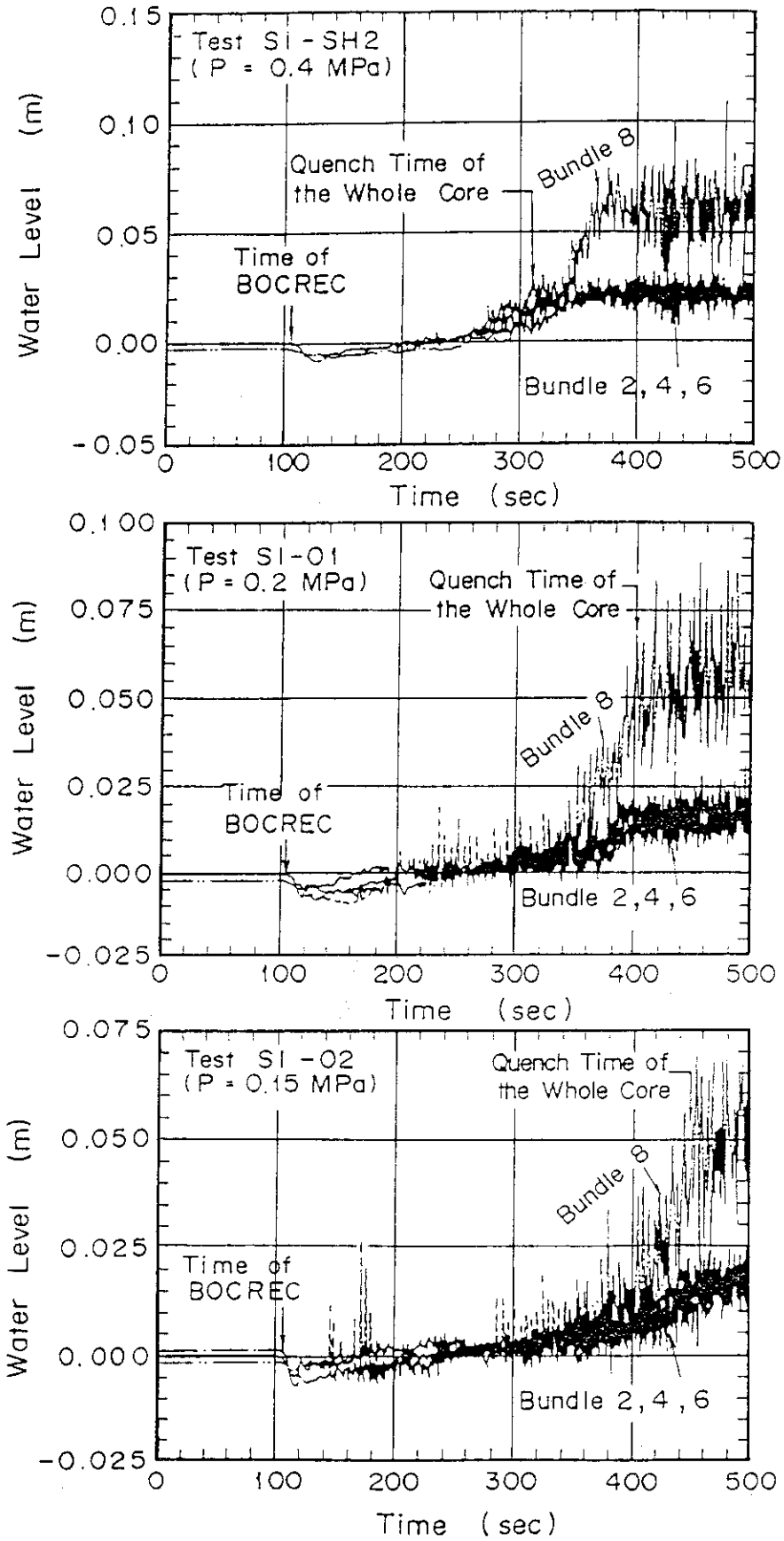

Fig. 27 Transients of Water Level in End Boxes above Bundle No's 2, 4, 6 and 8 in Tests S1-SH2(0.4MPa), S1-01(0.2MPa) and S1-02 (0.15MPa)

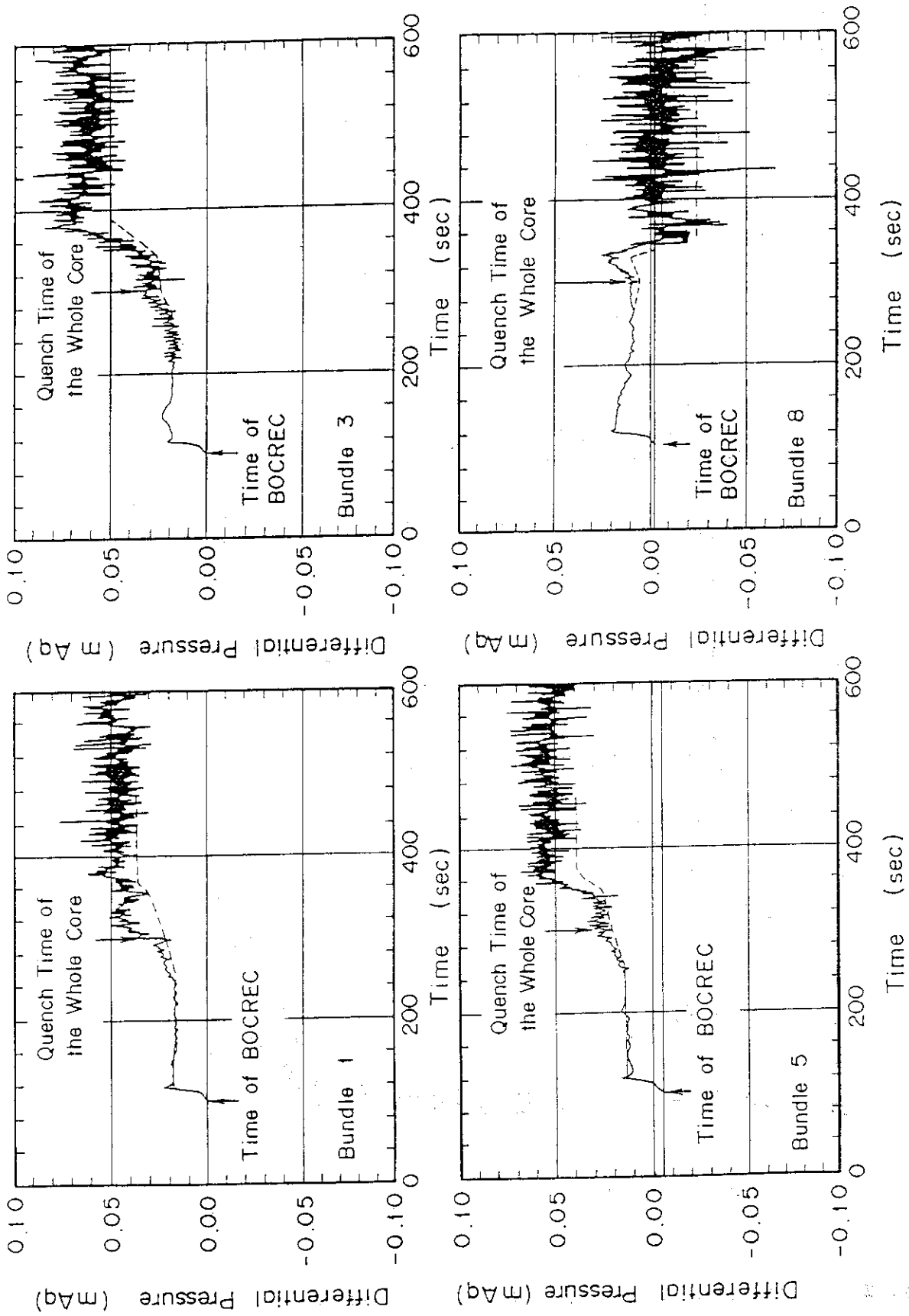

Fig. 28 Transients of Differential Pressure across End Box Tie Plates above Bundle No's 1, 3, 5 and 8 in Tests S1-SH2(0.4MPa), S1-01(0.2MPa) and S1-02(0.15MPa)

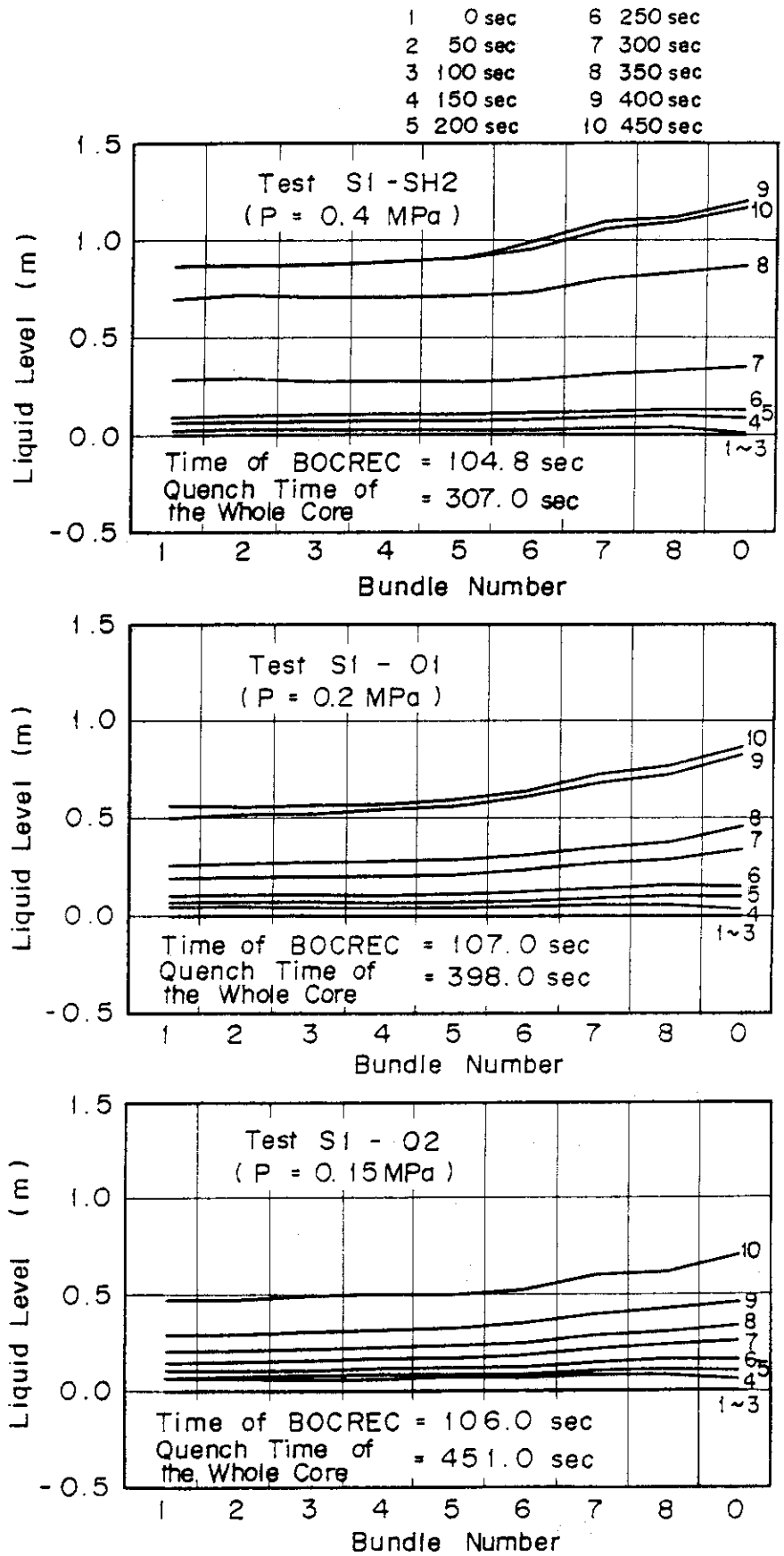

Fig. 29 Hosizontal Water Level Distribution on UCSP in Tests S1-SH2 (0.4MPa), S1-01(0.2MPa) and S1-02(0.15MPa)

付録　本文和訳

平板炉心再冠水試験・第1次模擬炉心試験結果

（系圧力の再冠水現象に及ぼす影響）

Ⅰ．緒　言

日本原子力研究所では，大型PWRの冷却材喪失事故（LOCA)時のブローダウン末期から，リフィル，再冠水過程にかけての，炉心内二次元熱水力挙動や，炉心の流体挙動と上部プレナムの流体挙動との間の相互干渉を研究するために，平板炉心試験装置（SCTF)を製作した。平板炉心試験計画は，米国，西ドイツおよび日本の間で結ばれた，いわゆる2D／3D協定に基いて進められており，SCTFと，西ドイツの上部プレナム試験装置（UPTF）とを組合せた結合実験も計画されている。

これらの目的のために，Fig. 1 に示すようにSCTF は，大型PWRの炉心の軸長を高さとし，半径を横巾とし，1バンドル巾を奥行とする平板状の部分を模擬するように設計されており，上部プレナム，下部プレナム，ダウンカマ等の対応する部分もそなえている。模擬圧力容器の内部構造はFig. 2 に示す通りである。さらに，Fig. 3 に示すように，実用PWRのものを単純化した模擬一次冷却系もそなえている。

模擬炉心は，一列に配置された8体の電気加熱式模擬燃料集合体からなり，炉心の最大出力は10MWである。それぞれの模擬燃料集合体の設計は基本的にはウエスチングハウス型の15×15本集合体の設計に準拠しているが，バンドル寸法は16×16本である。中心集合体模擬用のものから数えて第3および第4番目の模擬燃料集合体が，いわゆる閉塞燃料集合体であり，これらに属するすべての発熱棒の中央部に，燃料被覆管のふくれを模擬した鞘が取付けられている。

本報告においては，平板炉心第1次模擬炉心を用いた強制注入試験シリーズのうち，系圧力を変化させたS1－SH2（公称系圧力：0.4MPa），S1－01（0.2MPa）およびS1－02（0.15MPa）の3つの試験のデータに基いて，系圧力が再冠水現象に及ぼす影響について論ずる。これら3つの試験の主要な試験条件をTable 1～Table 3 に，また主な事象の発生時刻をTable 4 ～Table 6 にそれぞれ示す。

Ⅱ．主な結果

(1) システムの流体挙動

i）システム内の全体的な流体挙動を明らかにするためと，計測系の性能確認のために，システム各部の質量バランスの検討を行なった。その結果を，Fig. 4～Fig. 6 に示す。これらの図からわかるように，非常用炉心冷却系（ECCS）の注入水量と，圧力容器から流出する蒸気および水の量，および圧力容器に蓄積する水の量の和との間には，きわめて良い一致関係が見られ，本試

験の計測系の信頼性が全体として確認された。

ii）Fig. 7 に示すように，系圧力が低いほど，ホットレグのキャリオーバ水量は大きい。これは蒸気の比体積が大きいため，蒸気流速が速くなり，それがキャリオーバ現象に効いて来るものと考えられる。

(2) 炉心の熱的挙動

i）クエンチの進行や，被覆材温度のターンアラウンド挙動など，炉心の全体的な熱的挙動を検討した。模擬燃料棒の被覆管温度挙動の測定例をFig. 8に示す。

Fig. 9 ～Fig. 11に示すように，系圧力が高いほど，クエンチ時刻は早くなり，クエンチ温度は高くなり，ターンアラウンド時刻は早くなる。このような特性は，特に炉心の中・下部で明らかに見られる。しかし，Fig. 12に示すように，ターンアラウンド温度は余り変らない。ターンアラウンド温度が余り変らなかった理由の1つとして，これら3つの試験ではBOCREC（再冠水開始）時の被覆材温度がほゞ等しく設定されており，かつBOCRECからターンアラウンドまでの温度上昇そのものが小さかったことが挙げられる。

ii）Fig. 13，Fig. 14 に示すように，炉心上部では上方から下方へのクエンチの進行が見られたが，それ以外の場所では，クエンチは下方から上方へ進行した。

上方から下方へのクエンチの進行はランダムな現象であり，多くの熱電対で，同じ高さに取付けてある他の熱電対よりも早いクエンチが観測された。上方から下方へのクエンチの進行は，おそらく，炉心のより下の部分からとばされて来る液滴や，上部プレナムから流下して来る液膜の冷却効果によるものである。上方から下方へ進行するクエンチについては，非発熱棒や上部プレナム構造物の配置の，クエンチ時刻に及ぼす影響が認められた。

iii）下方から上方へのクエンチの進行については，Fig. 15，Fig. 17 に示すようにわずかではあるが，炉心半径方向出力分布の，クエンチ時刻やターンアラウンド温度に及ぼす影響が認められた。しかし，Fig. 16に示すように，クエンチ温度は余り影響を受けなかった。

また，流路閉塞模擬のために発熱棒に取付けた鞘のクエンチ挙動に対する影響は認められなかった。

iv）Fig. 18 に示すように，炉心のあらゆる場所で，クエンチ時刻の円周方向分布が認められ，スラブ壁が吸熱源となっていることが示唆される。SCTFと違って，実用PWRにはこのようなスラブ壁がないので，この事については，今後定量的に検討する必要がある。

v）下方から上方へのクエンチの進行速度のデータは，Fig. 19に示すように系圧力が高い時は村尾[1]の相関式とほゞ一致した。

村尾の相関式と試験結果とでは系圧力の影響の程度が全く違っており，このため，系圧力が低い場合には計算値と実測値の差が拡大した。なお，本試験の試験条件は村尾の式の適用範囲を外れていることが指摘される。特に冠水速度が小さく，クエンチ温度が低いことが問題であると考えられる。

(3) 炉心熱伝達

i）Fig. 20 に示すように，同時刻について比較すれば，系圧力が高いほど，発熱棒表面の熱伝達率および熱流束の値は大きかった。

ii）Fig. 20に示すように，膜沸騰熱伝達率に関する数土[2]の相関式は，クエンチ上流側の熱伝達率の値をやゝ大きめに評価しているものの，本試験結果と比較的よく一致した。

(4) 炉心および圧力容器内の二次元流体挙動

i）炉心出入口差圧の水平方向分布（Fig. 21），炉心部の水平方向差圧（Fig. 23），炉心流体密度の水平方向分布（Fig. 24～Fig. 26），エンドボックス水位（Fig. 27）および差圧（Fig. 28）の水平方向分布，上部炉心板上の水位の水平方向分布（Fig. 29）など，多くのデータに，二次元性が確認された。

ii）上記の二次元性は，それ自体の強さはそれほど強いものではないが，このことは必ずしも，炉心流速の水平方向成分の影響が小さいということを意味しない。例えば，Fig. 22に示すように，一次元の仮定の下に Cunningham－Yeh[3] のボイド率相関式を用いて炉心上下差圧の分布を計算したが，良い予測結果は得られなかった。このことは，炉心流速の水平方向成分による水平方向圧力分布の平担化があることを示唆するものである。

iii）Fig. 28に示すエンドボックスタイプレート差圧のデータは，炉心外周部を模擬する第8バンドルの領域で，下向きの水流（フォールバック）があることを示唆している。同様の現象は，隣接する第7バンドル領域でも見られた（データは示していない。）。

iv）第3，第4バンドルに取付けた被覆管のふくれを模擬するための鞘の，炉心二次元流体挙動に及ぼす影響については，本報の3つの試験に関する限り認められなかった。しかし，これらの試験は何れもいわゆる強制注入試験であるので，実用PWRの再冠水現象の重要な特性について見逃している可能性も考えられるから，本件に関する最終的結論は，将来コールドレグ注入試験を実施した後に出す予定である。

文　献

(1) Y. Murao, J. Nucl. Sci. Technol., 15〔12〕, 875～885 (1978)
(2) Y. Sudo, J. Nucl. Sci. Technol., 17〔7〕, 516～530 (1980)
(3) J. P. Cunninghan and H. C. Yeh, Trans. ANS, 17, 369～370 (1973)